R-11-28

# Rock support options for deposition tunnels

Henrik Ittner, Rolf Christiansson
Svensk Kärnbränslehantering AB

July 2017

**Svensk Kärnbränslehantering AB**
Swedish Nuclear Fuel
and Waste Management Co

Box 3091, SE-169 03 Solna
Phone +46 8 459 84 00

ISSN 1402-3091
**SKB R-11-28**
ID 1294716
July 2017

# Rock support options for deposition tunnels

Henrik Ittner, Rolf Christiansson
Svensk Kärnbränslehantering AB

*Keywords:* Deposition tunnel, Rock support, Tunnel maintenance, Shotcrete, Wire mesh, Numerical stress simulation, Thermal expansion, Spalling, Rock stress, TASS, KBP5002.

A pdf version of this document can be downloaded from www.skb.se.

# Preface

This report builds on a Master Thesis produced by Henrik Ittner at the department of Civil and Environmental Engineering, Chalmers University of Technology, Gothenburg titled “Support design for deposition tunnels”, Master Thesis 2011:87.

In addition to the authors, the following persons have contributed to this report. Eva Hakami (Geosigma AB) has conducted simulations of temperature loads in the two-dimensional finite difference code FLAC (version 7.00) developed by ITASCA Inc. Pär Kinnbom (3D-innovation AB) has prepared sections from the laser scanning of the TASS.

# Summary

The radioactive waste from nuclear power plants in Sweden is managed by the Swedish Nuclear Fuel and Waste Management Co, SKB. After interim storage the fuel will be placed in impermeable copper canisters and transported to a planned geological repository in the Forsmark area in the municipal of Östhammar. The canisters will be stored in a system of deposition tunnels at a depth of about 500 m according to the KBS-3 method.

A work environment risk for personnel working in the deposition tunnels are gravity or stress induced fall of blocks. This risk could be reduced or avoided by supporting the rock mass in locations were block falls are most likely to occur. Experience from Äspö Hard Rock Laboratory (HRL) indicates that work with heat producing machinery, for example the drilling of deposition holes, may affect the magnitude of induced stress around the excavation.

In the framework of this report numerical stress simulations of in plain induced stress during excavation and heating has been conducted with geometry sections from laser scanning of the experimental tunnel TASS in Äspö HRL using Forsmark rock mass properties. In addition this report compiles experience from tunnel maintenance and reinforcement in Äspö HRL

The results from the numerical stress simulations suggests that spalling and induced fracturing can be assumed to be less frequent if the in situ stresses in the Forsmark area corresponds to the most likely case. The heath simulations indicate that a 5 °C increase in temperature will, depending on the in situ stress situation, result in a ± 10 MPa stress change on the excavation boundary. If the induced stress on the excavation boundary is near the crack initiation limit of the rock the stress change from the temperature load can lead to failure and possible block fall.

Based on experience from Äspö HRL it should be possible to reach the requirements on stability and reinforcement by the Swedish Work Environment Authority (Arbetsmiljöverket) for the deposition tunnels with continuous maintenance scaling combined with selective rock support measures. This is also supported by the results of the numerical stress simulations.

A toolbox of support solutions should be established. The proposed support types must be able to protect the personnel working in the deposition tunnels as well as machinery from both types of outbreaks, i.e. both spot and surface support measures needs to be taken.

Due to the excavation method the rock support will in most cases be installed in end of the blast rounds. Reporting and documentation of observed fall of ground should always be performed and documentation of scaling activities must be carried out for each scaling occasion.

# Sammanfattning

Använt kärnbränsle från svenska kärnkraftverk hanteras av Svensk Kärnbränslehantering AB, SKB. Efter mellanlagring kapslas bränslet in i täta kopparkapslar och transporteras till ett planerat geologisk djupförvar för använt kärnbränsle i Forsmark, Östhammars kommun. Kopparkapslarna placeras på ett ungefärligt djup av 500 m i enlighet med KBS-3 metoden.

En arbetsmiljörisk för personalen som arbetar i deponeringstunnlarna är gravitationsdrivna eller spänningsinducerade blockutfall. Den här risken kan minimeras genom att förstärka bergmassan i de områden där flest blockutfall inträffar. Erfarenhet från Äspölaboratoriet indikerar att arbete med värmealstrande maskiner, till exempel under borrning av deponeringshål, påverkar den inducerade spänningsnivån runt tunnlarna.

Inom ramen för denna rapport har numeriska spänningssimuleringar av inducerad spänning vid uttag och uppvärmning i ett plan genomförts på sektioner från laserscanning av försökstunneln TASS i Äspölaboratoriet. För detta har mekaniska egenskaper från berget i Forsmark använts. Rapporten sammanställer också erfarenheter av bergförstärkning och bergunderhåll från Äspölaboratoriet.

Resultatet från de numeriska spänningssimuleringarna påvisar att sprickbildning och spjälkning kan antas i mindre omfattning förutsatt att in situspänningarna i Forsmark är lägre eller motsvarar det mest troliga fallet. Simulering av värmelast indikerar att en temperaturökning om 5 °C kan, beroende på in situ-spänningsfall, resultera i en spänningsförändring om ± 10 MPa på randen av tunneln. Om den inducerade spänningen ligger nära gränsen för sprickbildning kan den ökade spänningen leda till brott, vilket kan resultera i blockutfall.

Baserat på erfarenhet från Äspölaboratoriet är det möjligt att uppnå arbetsmiljöverkets krav för stabilitet och bergförstärkning med selektiv bergförstärkning kombinerat med återkommande underhållsskrotning. Detta stöds också av de numeriska spänningssimuleringarna.

Ett koncept med olika förstärkningslösningar bör tas fram. Föreslagen bergförstärkning för deponeringstunnlarna måste klara kravet att skydda personal och maskiner som arbetar i deponeringsområdet från både strukturkontrollerade och spänningsinducerade blockutfall, det vill säga både yt- och selektivförstärkning krävs.

På grund av drivningsmetoden kommer selektiv bergförstärkning i de flesta fall installeras i salvslut. Rapportering och dokumentation av blockutfall och skrotning skall därför alltid utföras.

# Contents

# 1 Introduction

## 1.1 Background

The radioactive waste from nuclear power plants in Sweden is managed by the Swedish Nuclear Fuel and Waste Management Co, SKB. After interim storage the fuel will be placed in copper canisters and transported to a planned geological repository in the Forsmark area in the community of Östhammar. The canisters will be deposited in the bedrock at a depth of about 470 m according to the KBS-3 method. The deposition will be carried out in a system of deposition tunnels. The canisters will be placed in vertical boreholes (Ø 1.8 m) embedded in highly compacted bentonite clay. After deposition, the deposition tunnels will be backfilled with bentonite-clay and sealed with concrete plugs.

The strategy of reinforcement for the deposition tunnels of the planned repository for spent nuclear fuel has only been studied in a general perspective. In the layout D2 it was estimated that due to the good rock quality in Forsmark and the short operational time before backfill (≤ 5 years) there was a limited need for rock support in the deposition tunnels (Eriksson et al. 2009). There is however several reasons to investigate this further. Although it is expected that the deposition tunnels can be excavated in rock with very good quality with few open fractures the risk for gravity induced block falls, risking to impact vehicles or personnel working underground cannot be unforeseen. A source for causing blocks with a potential to fall is excavation damage and poor blast results, especially local failure to meet demands on contour control. It is also observed that the area around an end of a blast round is subjected to the most significant blast damage (Olsson et al. 2009, Ittner 2009). Such conditions may cause risk for temperature induced popping and spalling during work with heat producing machinery (Andersson and Söderhäll 2001). There is also a need to develop support strategies for unexpected rock conditions or fractured rock mass in deformation zones.

A safe work environment is important during construction and operation of the deposition tunnels. Work in underground environment, are subjected to the rules of the Swedish Work Environment Authority (Arbetsmiljöverket). The current rules applicable for the deposition tunnel are found in AFS 2010:1.

A possible danger is gravity or stress induced block falls. The risk for fall of ground to hit personnel working in the deposition tunnels could be reduced or avoided by supporting the rock mass in locations were block falls are most likely to occur.

## 1.2 Objective

The objective of this report is to give recommendations on support principles and solutions for the deposition tunnels in the planned repository for spent nuclear fuel in Forsmark. The study is based on experience from tunnel maintenance and reinforcement in Äspö Hard Rock Laboratory (HRL). Support strategies for unexpected rock conditions or fractured rock mass in deformation zones are not discussed in this report.

# 2 Site conditions

## 2.1 Geological conditions at repository depth

The geological conditions in the Forsmark area are described in Stephens et al. (2007) and SKB (2009a).

The Forsmark area consists of crystalline bedrock formed between ca 1.89 and 1.85 Ga during the Svecokarelian orogeny. The target volume is located within a tectonic lens that developed more than 1 850 million years ago, when the rock units were situated at mid-crustal depths and were affected by variable degrees of ductile deformation. The current strain condition is a result of plate motion related to mid-Atlantic ridge push, in combination with glacial isostatic rebound following removal of the latest Weichselian ice sheet and crustal unloading. The bedrock inside the lens at the depths of the repository is relatively homogeneous whereas the lithology and deformation is more variable outside the lens.

Figure 2-1 depicts the regional setting of structural geology in the Forsmark area. The location of regional deformation zones and areas subjected to ductile strain are noted in the figure.

The tectonic lens is divided into two rock domains, RFM029 and RFM045, were RFM029 is dominated by medium-grained metagranite-granodiorite. RF045 consists mainly of aplitic metagranite and subordinately of medium-grained metagranite-granodiorite. It is distinguished from rock domain RF029 by the widespread occurrence of fine-grained, albitized granitic rock, with higher contents of quartz compared to unaltered granitic rock.

A division of the bedrock between deformation zones into six fracture domains, FFM01 to FFM06, has been conducted based on an assessment of the variation in the frequency of particularly open and partly open fractures with depth along investigation boreholes

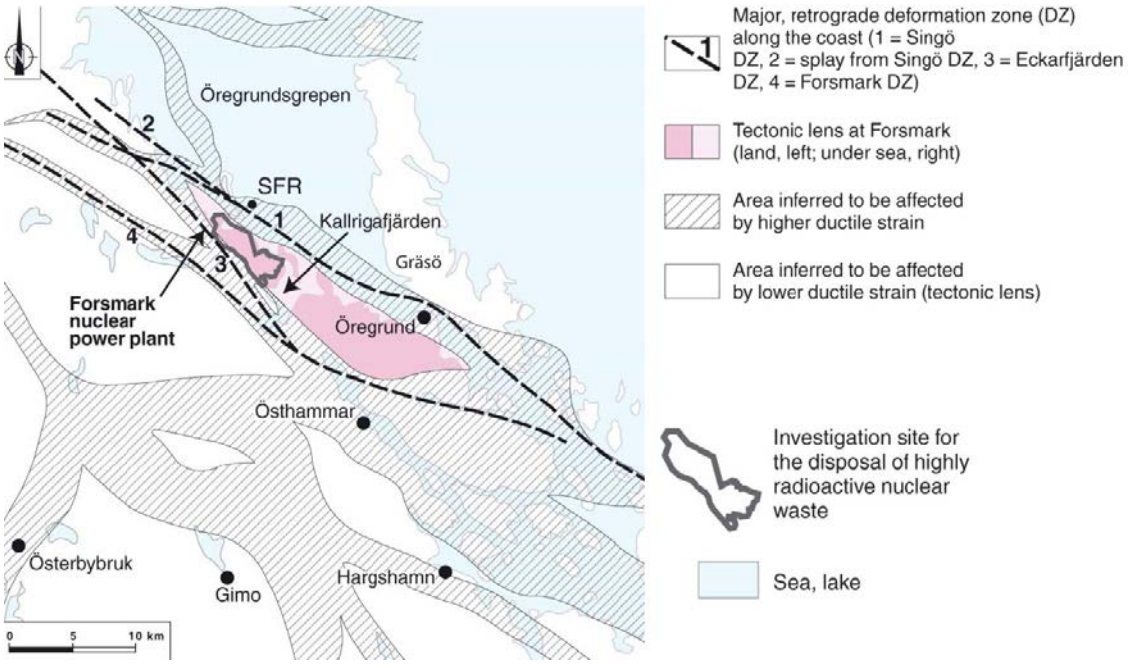


***Figure 2-1***. *Deformation zones: 1= Singö DZ, 2 = Splay from Singö, 3 = Eckarfjärden DZ, 4 = Forsmark DZ. Modified from Stephens et al. (2007).*

The distribution of the two rock domains and fracture domains at repository level are depicted in Figure 2-2 together with deformation zones longer than 1.000 m. The deformation zones are generally of three types (SKB 2009a):

1. Longer deformation zones, with steep dip and WNW to NW strike, located mostly outside the lens. These zones show both ductile and brittle deformation. The regional Forsmark and Singö deformation zones are both members of this set and form the boundary of the candidate volume.

2. Vertical and steeply-dipping, brittle deformation zones with NE to NNE strike. This set intersects the deposition area. It is strongly dominated by sealed fractures and sealed fracture networks. Alteration is present in the form of red staining. Cohesive breccia, cataclasite and quartz dissolution is also locally present. The thickness of the zones in the ENE to NNE set is estimated to be in a range between 2 and 45 m, influence on the excavation works is however considered to be limited. The deformation zone ZFMNE0060, that intersects the target area, is a member of this set.

3. Less extended brittle deformation zones with gentle dip relative to the other two sets. These zones contain an increased frequency of open fractures. Deformation zone ZFMNE00A2 is one of these prominent gently dipping deformation zones in the area located south and above the planned repository.

The construction experiences from nearby discharge tunnels from power plants and the SFR facility indicates that the geotechnical properties of the minor deformation zones have very minor impact on construction works (Carlsson and Christiansson 2007).

The fracture domains represented at repository depth are FFM01 and FFM06. Fracture domain FFM01 is located in the rock domain RFM029 inside the tectonic lens. It consists of vertical or steeply dipping fractures striking ENE to NNE and NNW, as well as gently dipping to sub-horizontal fractures. The experience at the SFR Facility suggests that sub-horizontal fractures may appear locally and of limited areal extent. Little difference in fracture frequency is expected between the rock mass in FFM01 and FFM06.

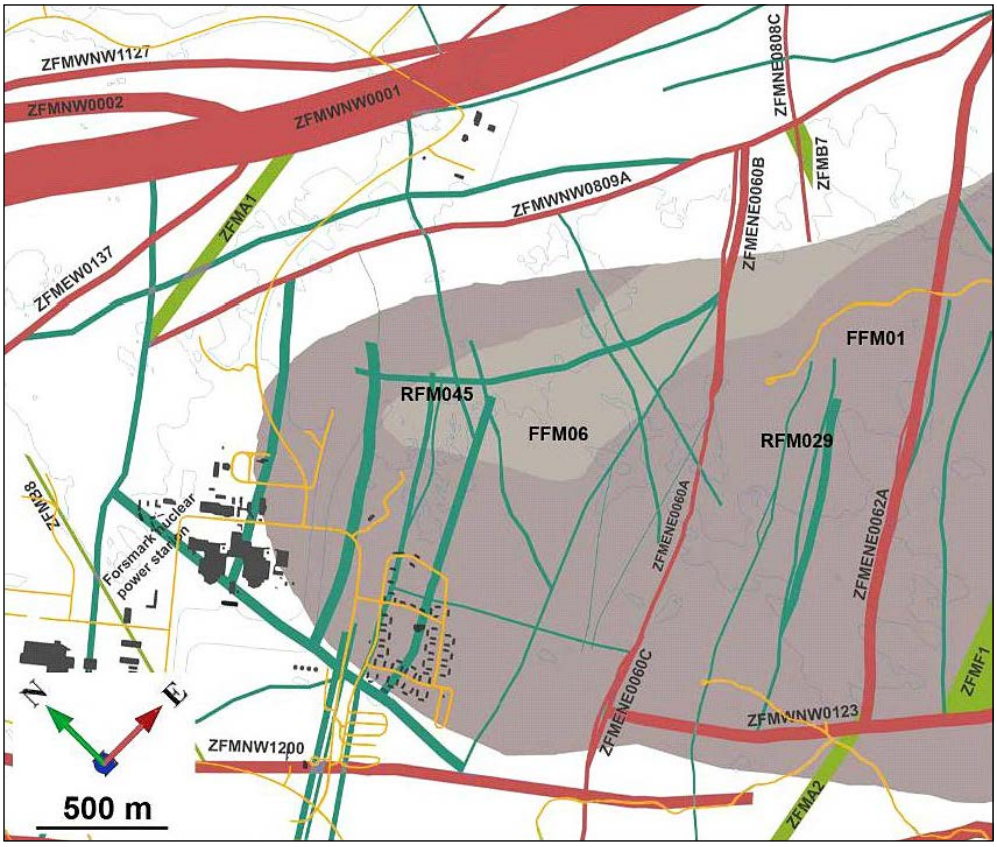


***Figure 2-2.*** *Distribution of the two rock domains RFM029 and RFM045, and all deformation zones at 500 meter depth. FFM01 and FFM06 are the corresponding fracture domain at this depth. Modified from SKB (2009a).*

Fracture domain FFM06 is situated within rock domain RFM045. Two sets of vertical or steeply dipping fractures that strike NE to NS and NW to WNW, as well as gently dipping to sub-horizontal fractures are located in this domain.

Fracture minerals are dominated by chlorite, calcite, adularia, hematite, laumontite and quartz. Epidote is relatively uncommon along the fractures in FFM06. The more common mineral laumontite is predominantly found along the steeply dipping NE to N-S fractures. However, some occurrences are also present along the fractures with other orientations. Clay minerals are present in both the steeply and gently dipping fractures.

Figure 2-3 depicts the location, typical fracture orientation and mineralogy for four of the six fracture domains. There is a significant difference in frequency of sub-horizontal fractures between the surface near domains FFM02 and FFM03 compared to the deeper FFM01 and FFM06. The possible difference in fracture frequency between fracture domains FFM01 and FFM06 is less pronounced. It is assumed in this study that the fracture distribution is rather similar all through the deposition area, but the distribution is heterogeneous. An estimated frequency of the open fractures that has largest impact on risk for fall of ground is shown in Figure 2-4.

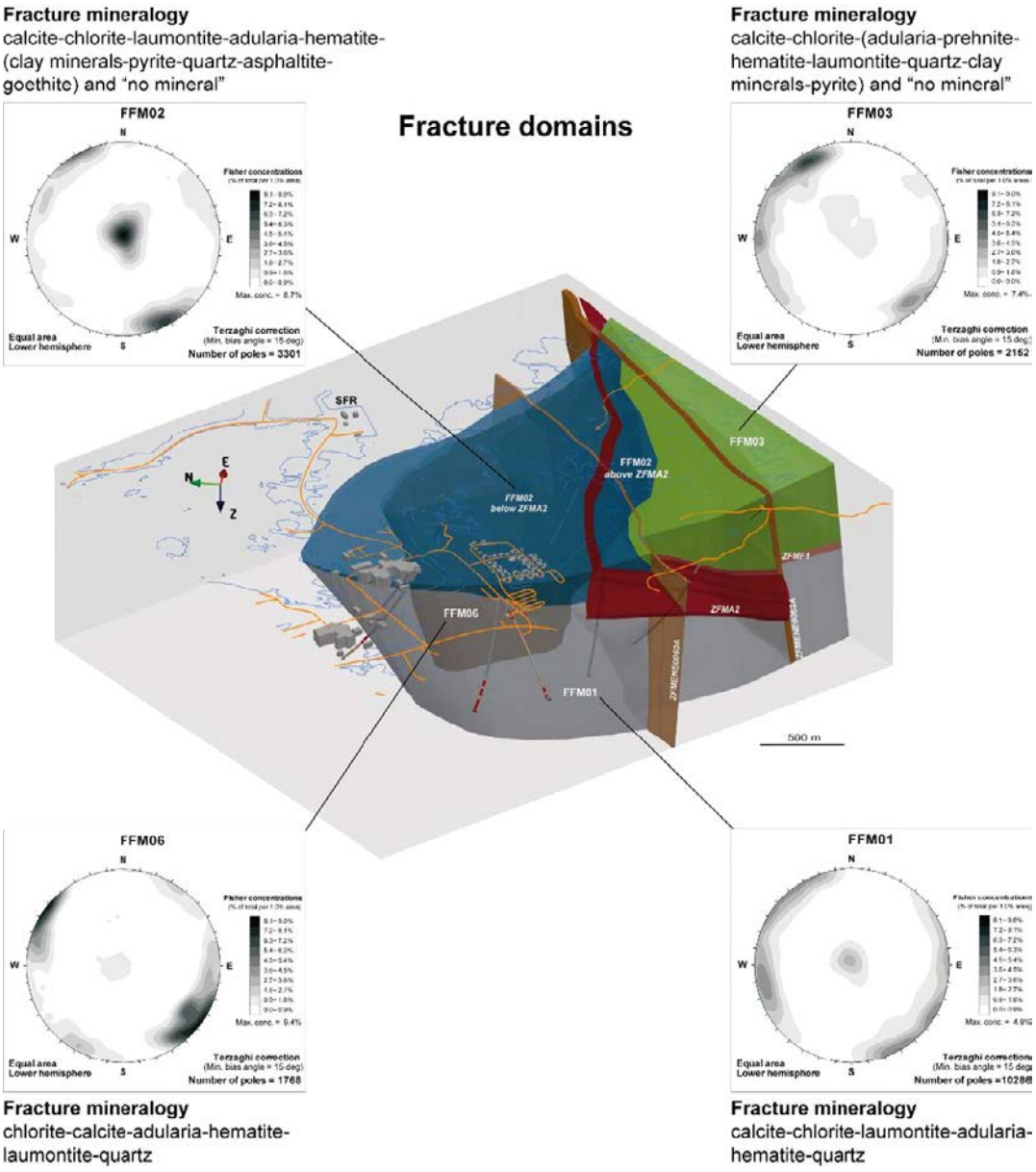


***Figure 2-3***. *Location, typical fracture orientation and mineralogy for four of the six fracture domains. Note the difference in frequency of sub-horizontal fractures between the surface near domains FFM02 and FFM03 compared to the deeper FFM01 and FFM06 (SKB 2009a).*

In order to translate the geological data from the geological model of the target volume into engineering terms, four ground types (GT) was defined in SKB (2009a). A summary of the ground types are presented in Table 2-1.

The ground types are based on experience from underground construction works in Forsmark, documented in the construction experience report (Carlsson and Christiansson 2007) and modern day construction experience in Scandinavia.

**Table 2-1. The four ground types (GT) was defined in SKB (2009a).**

| Ground type | Q-value | RMR-value | Description |
|---|---|---|---|
| GT1a | > 100 | 85–95 | Massive to sparsely fractured rock mass in RFM029 (FFM01). |
| GT1b | > 100 | > 90 | Massive to sparsely fractured rock mass in RFM045 (FFM06). |
| GT2 | 40–100 | 80–90 | Blocky rock mass. Moderately fractured rock contains fractures and hairline cracks, but the blocks between joints are intimately interlocked. (FFM02). |
| GT3 | 10–40 | 75–85 | Deformation zone containing sealed fracture network, fault breccias and cataclasite. |
| GT4 | 4–20 | 70–80 | Regional deformation zone, containing fault breccias, crushed rock, sealed networks and cataclasite. |

## 2.2 Hydro-geology and fracture system

The upper 150 to 200 m of the bedrock in Forsmark (Fracture domain FFM02) contains a relatively high frequency of sub-horizontal fractures or sheet planes, likely related to crustal unloading through erosion of overlaying sediments or melting of the Pleistocene ice sheets (Stephens et al. 2007). Sub-horizontal fractures, together with gently and steeply dipping sets, create a well-connected network of fractures which allows flow of ground water in the bedrock.

At repository depth the frequency of open fractures are lower. A trend with decreasing frequently of open fractures with depth can be identified from fracture statistics, Figure 2-4.

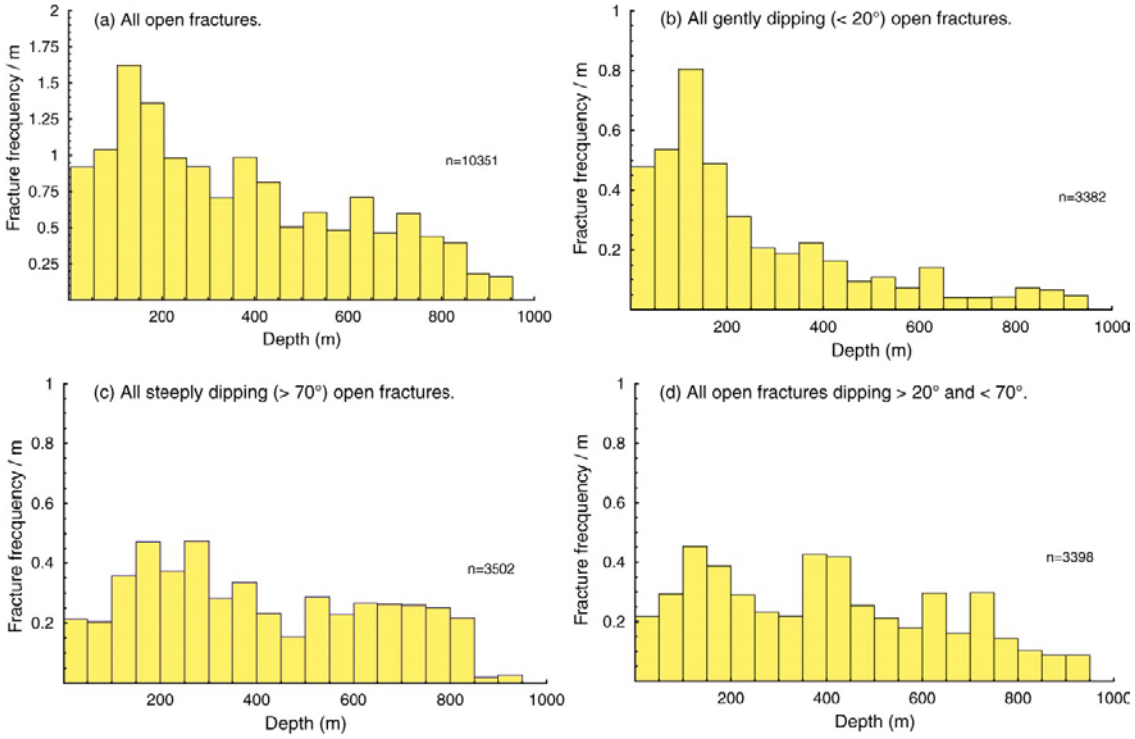


***Figure 2-4.*** *All open fractures from boreholes in Forsmark, visible in the BIPS log. Note the decrease in frequency with depth of sub-horizontal fractures (Martin 2007).*

Note that the trend with decreasing fracture frequency is strongest among sub-horizontal fractures. The decrease in frequency of horizontal fractures with depth gives a less connective fracture system at repository level.

Stigsson (2009) investigated the frequency of fractures assumed to be water conductive, i.e. open or partly open and directly or indirectly connected to a source. The tunnels and deposition holes were modelled as scanlines which is a very coarse approximation, but it may give some rough estimation of the frequency of the water bearing features, especially for the larger ones, and the total transmissivity in a section. The frequency of water bearing fractures was found to be very low at repository depth, and the transmissivities are also very low. It is therefore assumed in this study that ground water pressure at depth will not play any significant role in estimating of the stability of deposition tunnels and that need for pre-grouting will be limited.

## 2.3 State of in situ stress

The state of horizontal in situ stress in the target area is influenced by large scale tectonics and isostatic uplift of the crust. Brittle or ductile deformation of the bedrock and properties of the rock mass can locally influence the in situ stress orientation and magnitudes.

Martin (2007) gives a comprehensive analysis of the in situ stress conditions in the bedrock in Forsmark down to the depth 1 000 m. The analysis was conducted for the depth ranges 0–150 m, 150–400 m and 400–600 m based on results from overcoring (OC) and hydraulic fracturing (HF). Figure 2-5 shows the interpretation of the in situ stress state at 500 m depth.

The horizontal stress varies linear with the depth in ranges as the upper parts of the bedrock are subjected to more brittle deformation. It is therefore necessary to apply a linear formula for the in situ stress magnitude in each range. Table 2-2 presents the results of the in situ stress analysis for the depth ranges 0–150 m, 150–400 m and 400–600 m.

**Table 2-2. Results of the in situ stress analysis for the depth ranges 0–150 m, 150–400 m and 400–600 m, z is the depth below ground surface in meters (Martin 2007).**

| Depth range [m] | $\sigma_H$ [MPa] | Trend [°] | $\sigma_h$ [MPa] | Trend [°] | $\sigma_V$ [MPa] |
|---|---|---|---|---|---|
| 0–150 | 19 + 0.008z | 145 | 11 + 0.006z | 055 | 0.0265z |
| 150–400 | 9.1 + 0.074z | 145 | 6.8 + 0.034z | 055 | 0.0265z |
| 400–600 | 29.5 + 0.023z | 145 | 9.2 + 0.028z | 055 | 0.0265z |

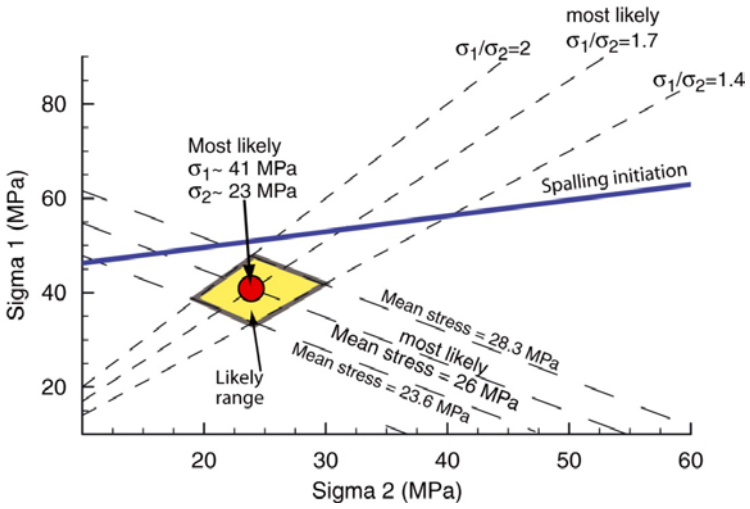


***Figure 2-5.*** *The range of magnitude for the likely and the most likely magnitude of the horizontal in situ stress state at the depth 500 m. The major horizontal in situ stress is denoted $\sigma_1$ and the minor in situ stress is denoted $\sigma_2$ in the figure. Spalling initiation is noted with a blue line in the figure. Note the most likely magnitudes $\sigma_1$= 41 MPa and $\sigma_2$ = 23 MPa (Martin 2007).*

A maximum stress magnitude has been determined from overcoring measurements, this represents the worst case scenario, Table 2-3 (SKB 2009a).

**Table 2-3. Maximum stress magnitude that represents the worst case scenario (SKB 2009a).**

| Depth [m] | $\sigma_H$ [MPa] | $\sigma_h$ [MPa] | $\sigma_V$ [MPa] |
|---|---|---|---|
| 500 | 62 | 43 | 13 |

## 2.4 Mechanical rock properties

The mechanical properties of the intact rock and rock mass in Forsmark have been analyzed and discussed in Glamheden et al. (2007). Table 2-4 presents a summary of the evaluated properties of intact rock in the Forsmark area.

**Table 2-4. Properties of intact rock in the Forsmark area (Glamheden et al. 2007).**

| Fracture domain | Rock code | Rock type | E-Modulus [GP] | Poisson's ratio v [–] | Friction angle φ [°] | Cohesion c [MPa] | Tensile strength $\sigma_t$ [MPa] | UCS $\sigma_c$ [MPa] |
|---|---|---|---|---|---|---|---|---|
| FFM01 | 101057 | Granite to granodiorite | 76 ± 3 | 0.23 ± 0.04 | 60 | 28 | 13 ± 2 | 226 ± 28 |
| FFM01 | 101061 | Pegmatite, pegmatitic granite | 75 ± 3 | 0.3 ± 0.03 | 56 | 33 | 12 ± 3 | 228 ± 21 |
| FFM06 | 101058 | Granite aplitic | 83 ± 8 | 0.27 ± 0.03 | 60 | 30 | 18 | 310 ± 58 |

Crack initiation strength $\sigma_{ci}$ is an indicator when stress induced spalling can occur. The $\sigma_{ci}$ has been evaluated from uniaxial compressive tests. Table 2-5 presents mean, min and max values for crack initiation for different rock types in the rock domains RFM029 and RFM045. The high value for crack initiation in RFM045 is most likely due to the higher quartz content in the aplitic granite (Stephens et al. 2007).

Based on laboratory tests on samples of intact rock and theoretical calculations an estimation of the mechanical parameters of the rock mass was conducted by Glamheden et al. (2007). Table 2-6 presents the rock mass properties for the Fracture domains FFM01 and FFM06.

**Table 2-5. Mean values for crack initiation for different rock types in the rock domains RF029 and RF045. Note the higher value for crack initiation in RFM045 (Glamheden et al. 2007).**

| Rock domain | Rock code | Rock type | Mean crack initiation strength $\sigma_{ci}$ [MPa] | Min crack initiation strength $\sigma_{ci}$ [MPa] | Max crack initiation strength $\sigma_{ci}$ [MPa] |
|---|---|---|---|---|---|
| RFM029 | 101057 | Granite to granodiorite, metamorphic, medium-grained | 115 ± 21 | 60 | 187 |
| RFM029 | 101061 | Pegmatite, pegmatitic granite | 123 ± 12 | 100 | 140 |
| RFM045 | 101058 | Granite, metamorphic, aplitic | 169 ± 29 | 125 | 200 |

**Table 2-6. Rock mass properties for the fracture domains FFM01 and FFM06 (Glamheden et al. 2007).**

| Fracture domain | Deformation modulus E [GP] | Poisson's ratio v [–] | Friction angle φ [°] | Tensile strength $\sigma_t$ [MPa] | UCS $\sigma_c$ [MPa] |
|---|---|---|---|---|---|
| FFM01 | 70 ± 8 | 0.24 ± 0.03 | 51 ± 2 | 2.4 ± 1 | 92 ± 27 |
| FFM06 | 69 ± 12 | 0.27 ± 0.04 | 51 ± 2 | 2.3 ± 1 | 95 ± 32 |

## 2.5 Thermal rock mass properties

A model of the thermal properties of the bedrock in Forsmark has been established by SKB in several steps. Some of the results, relevant to this report are presented in Sundberg et al. (2005, 2008) and Stephens et al. (2007).

Fluctuation in temperature will alter the radial and tangential stresses around an excavation. A change in temperature $\Delta T$ will induce a strain $\varepsilon_T$ in the rock mass. The magnitude of the strain $\varepsilon_T$ is dependent on the coefficient of thermal expansion $\alpha$. Increased temperature in the rock material will force a higher stress and decreased temperature will lead to relaxation.

$$\varepsilon_T = \alpha \cdot \Delta T \quad 2\text{-}1$$

$$\sigma_T = E \cdot \varepsilon_T \quad 2\text{-}2$$

The coefficient of thermal expansion $\alpha$ has been measured on samples from the Forsmark area. The values for three different rock types are presented in Table 2-8.

**Table 2-8. The coefficient of thermal expansion α for some the rock types in Forsmark (Sundberg et al. 2005).**

| Rock code | Rock type | α [m/mK] |
|---|---|---|
| 101057 | Granite to Granodiorite | $7.7 \times 10^{-6} \pm 2.2 \times 10^{-6}$ |
| 101054 | Tonalite to Granodiorite | $7.2 \times 10^{-6} \pm 1.6 \times 10^{-6}$ |
| 101051 | Granite, Granodiorite and Tonalite | $8.2 \times 10^{-6} \pm 1.8 \times 10^{-6}$ |

No domain model have been evaluated for the coefficient of thermal expansion and the mean value for the most common rock type (Granite to Granodiorite, 101057) can be used for the rock domain RFM029 **(**Sundberg et al. 2005).

The thermal conductivity and heat capacity of the rock has been assessed from direct measurements and by calculations based on mineral composition. Direct measurements were performed on the dominating granite. The values for the other rock types are calculated, Table 2-9 and Table 2-10. For more details see Sundberg et al. (2008) and Back et al. (2007). Note that heat capacity is less sensitive to the evaluation scale compared to heat conductivity.

**Table 2-9. Mean thermal conductivity for the two rock domains at repository level. The values are based on calculations from TPS measurements and evaluated at 5m scale (Sundberg et al. 2008) and (Back et al. 2007).**

| Rock domain | Mean thermal conductivity [W/m·K] at approx. 20 °C | Mean temperature dependence [%] per 100 °C |
|---|---|---|
| RFM029 | 3.57 ± 0.13 | 10 |
| RFM045 | 3.56 ± 0.28 | 10 |

**Table 2-10. Mean heat capacity for the two rock domains at repository level. The values are based on calculations from TPS measurements and evaluated at 1 m scale (Sundberg et al. 2008).**

| Rock domain | Mean heat capacity [MJ/m³·K] at approx. 20 °C | Mean temperature dependence [%] per 100 °C |
|---|---|---|
| RFM029 | 2.06 ± 0.1 | 29 |
| RFM045 | 2.12 ± 0.15 | 29 |

# 3 Proposed layout

## 3.1 Deposition area

Based on the geological situation in the target area, the deposition area is proposed to be located in the rock domains RFM029 and RFM045 with respect distance to some of the deformation zones (SKB 2009b). The deformation zones which require a respect distance are ENE060A, ENE062A and NW0123. Figure 3-1 shows the location of the available deposition area bounded by the respect distance to major deformation zones.

Several minor deformation zones are located within the deposition area, see deformations zone of type three and Figure 2-2 in Chapter 2.

## 3.2 Deposition tunnel design and layout

In order to minimize horizontal in situ stress acting on the deposition tunnels and the induced tangential stress and risk for spalling in the tunnel roof and deposition holes, the deposition tunnels will be oriented sub-parallel (± 30 °C) to the maximum horizontal in situ stress. Figure 3-2 shows the location and orientation of the main, transport and deposition tunnels relative to the rock domains RFM029 and RFM045 and to the orientation of major horizontal in situ stress.

Figure 3-3 shows the proposed theoretical section of a deposition tunnel, with height 4.8 m and width 4.2 m. According to SKB (2009a) deposition tunnels may not be longer than 300 m due to safety in case of hazards, e.g. fire.

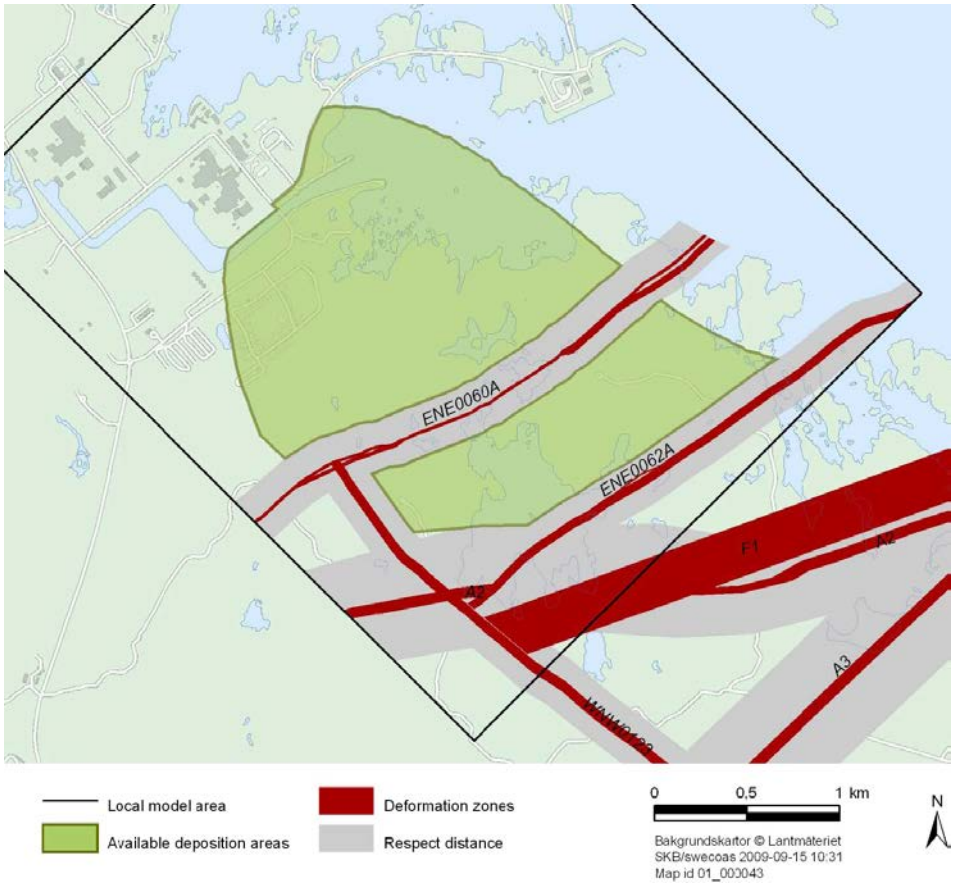


*Figure 3-1. Location of the available deposition area bounded by the respect distance to major deformation zones. Modified from SKB (2009b).*

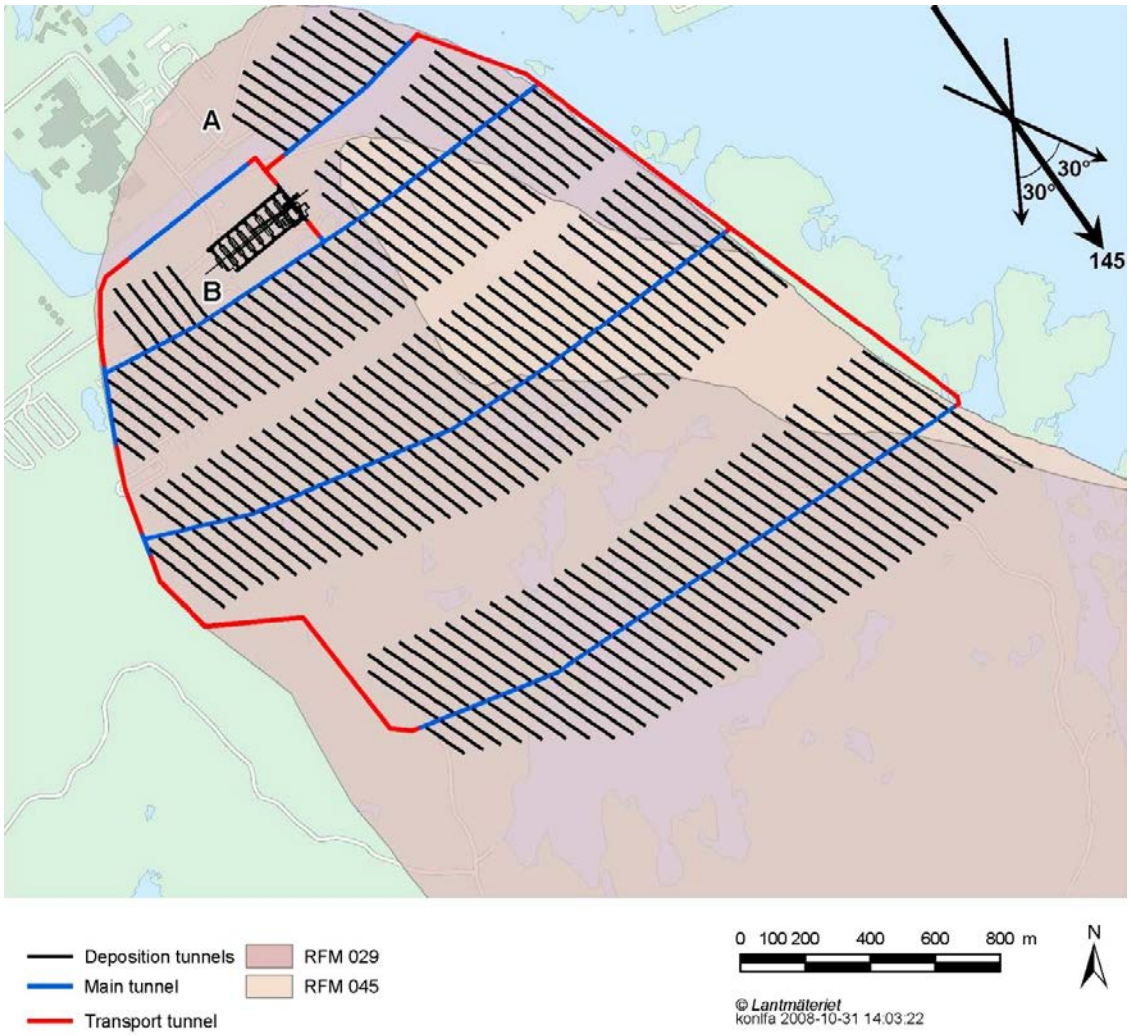


***Figure 3-2.*** *Location and orientation of the main, transport and deposition tunnels relative to the rock domains RFM029 and RFM045. The orientation of major horizontal in situ stress is noted to the upper right in the figure. Modified from SKB (2009b).*

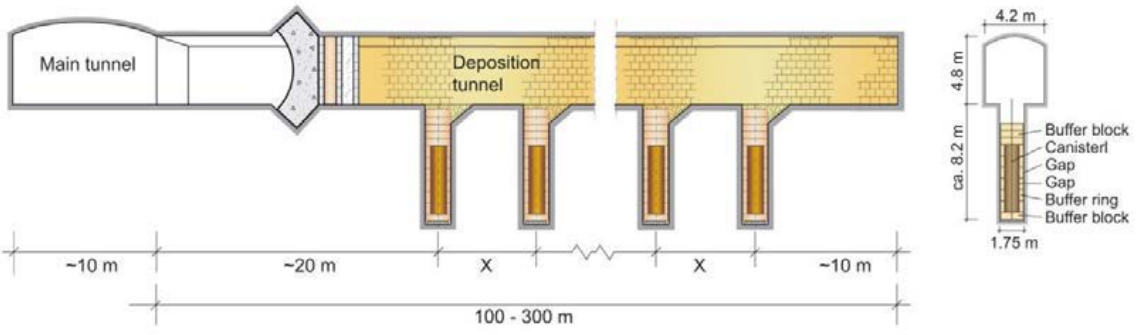


***Figur 3-3.*** *Proposed theoretical section of a deposition tunnel, with height 4.8 m and width 4.2 m.*

## 3.3 Excavation method and expected non-conformities

The deposition tunnels will be excavated with drill and blast technology. A part of this technology is that the excavated tunnel contour deviates from the theoretical tunnel contour due to the look-out angel required by the drilling rig. The deviation reaches the largest magnitudes in the end of the blast rounds, Figure 3-4.

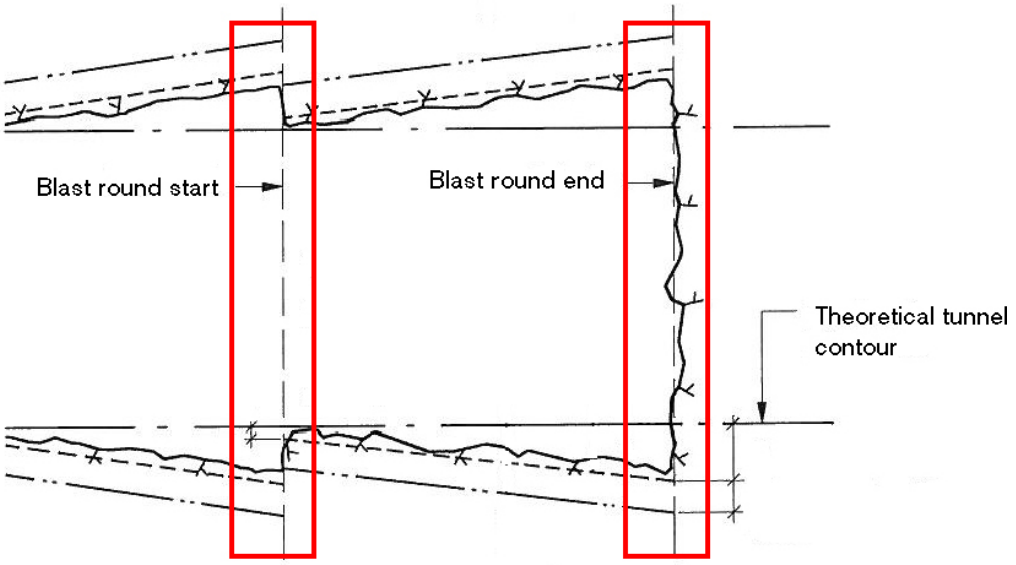


***Figure 3-4.*** *Plan of a tunnel section excvated with drill and blast techniqe. Note the deviation between excavated and theoretical contour. The end of the blast rounds, were most of the blast damage is located are are marked in the figure. Modified from Svensk byggtjänst (1999, pp 41–51).*

The geometrical deviation and heavier explosives used in the end of the blast rounds may lead to overbreak and blast damage.

The experimental tunnel TASS, located in Äspö HRL at the −450 m level, has a geometry similar to the deposition tunnels. The main purpose of the tunnel was to conduct a full scale test of grouting technology, using silica sol, and to apply an excavation method that focused to minimize overbreak, blast damage and extension of the excavation damage zone (EDZ).

The backfill procedure and the risk for water leakage through damaged rock mass puts high demands on the geometry, contour and EDZ for the deposition tunnels. Those demands were applied during the excavation of TASS. The aim was to accomplish the following requirements for contour and overbreak (Karlzén and Johansson 2010).

1. The tunnel contour was not allowed to be smaller than the theoretical contour, i.e. 4.2 m.
2. The overbreak was not allowed to exceed 30 % in each blasting round.
3. No remaining rock inside the theoretical contour.
4. Deviation from theoretical contour in the end of blast rounds in the tunnel roof: 20 cm.
5. Deviation from theoretical contour in the end of blast rounds in the tunnel floor: 25 cm.

Demands for drilling, loading and blasting design were set after those requirements.

The tunnel was excavated in stages with 2 to 4 rounds in each stage. In total 20 rounds were excavated in 6 stages.

All of the demands were more or less successfully fulfilled. The small amount of remaining rock inside the theoretical contour could be removed with for example mechanical scaling. There were no significant difference in overbreak between 20 and 25 cm deviation from theoretical contour in the end of blast rounds, the volumes differ 1.5 %.

The project was carefully planned in order to allow time for observation, reflection and feedback. This has resulted in a good quality of the excavated tunnel.

During 2008 and 2009 a full 3D laser scanning of the TASS tunnel was conducted. The scanning of the TASS and some general principles of laser scanning are described by Hardenby and Sigurdsson (2010) and Karlzén and Johansson (2010). A second laser scanning was performed in May 2011. Figure 3-5 depicts a model of the TASS based on the laser scanning conducted in 2009.

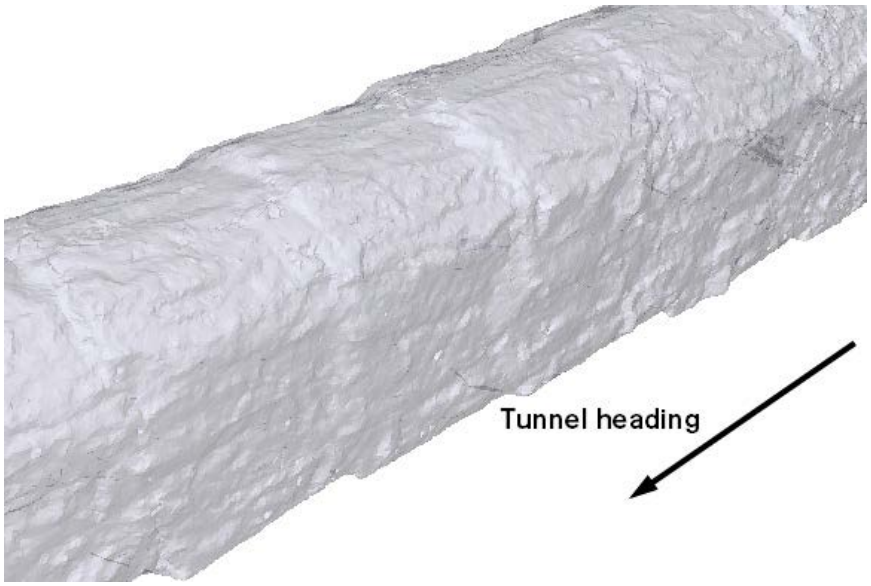


***Figure 3-5.*** *Laser scanned model of the TASS with marked heading. Note the deviations in tunnel shape at the end of the blast rounds. Figure by Pär Kinnbom (modified).*

## 3.4 Anticipated rock mechanical problems

Mapping of instabilities and simulation of induced stress around the TASS tunnel identified three possible main failure modes for a deposition tunnel in a rock mass corresponding to GT1 (Ittner 2011):

1. Cracking or spalling resulting from high induced stresses around the excavation. A change in the stress conditions by heat producing machinery or other activities in the tunnel can also trigger thermal induced spalling.
2. Gravity driven falls of wedges resulting from intersecting fractures and low stresses or tension.
3. Blocks loosening due to relaxation resulting from blast damage or geological fractures. These blocks can currently be stable but there is a potential risk for falling due to creep or change in boundary conditions such as temperature or humidity.

Gravity driven loose block or wedges will most likely require spot bolting. A rough contour leads to local stress concentrations as well as unloading. If the induced stress exceeds the crack initiation limit, the risk for cracking and spalling is increased. However if there are indications of low stress or tension in a section a loose block is no longer confined by the induced stress. This is most frequently the situation in the tunnel walls. The presence of geological fractures is a condition for the structural failure types to occur. High density of natural fractures, several fracture sets and unfavorable fracture orientation increases the risk for an uneven contour as the blasting gases can penetrate the fractures and force the breakage to occur in the natural fractures. The annual variation in temperature and humidity could also be a driving force to loosen up the rock surface during operation of the repository.

The main activities in the deposition tunnels after excavation will be drilling of deposition holes, deposition of canisters and backfilling. During these activities a possible block fall may occur due to change in moisture or temperature.

In order to evaluate rock mechanical behaviour in the repository three categories of ground behaviour (GB) has been defined by SKB in SKB (2009a). The expected ground behaviour types in the deposition area are GB1 and GB2A, where GB1 is the dominating ground behaviour type. GB2B is expected to be limited to minor deformation zones. Table 3-1 presents an overview of ground behaviour types.

**Table 3-1. Description of the ground behaviour types defined. Modified from SKB (2009a).**

| Ground behaviour | Description |
|---|---|
| GB1 | Gravity driven, mostly discontinuity controlled failures (block falls), where pre-existing fragments or blocks in the roof and sidewalls become free to move once the excavation is made. |
| GB2 | Stress induced, gravity assisted failures caused by overstressing, i.e. the stresses developed in the rock reaching the local strength of the material. These failures may occur in two main forms:<br>A) Spalling, buckling or rock burst in materials with brittle properties, i.e. massive brittle rocks.<br>B) Plastic deformation, creep, or squeezing in materials having ductile or deformable properties, i.e. massive, soft/ductile rocks or particulate materials (soils and heavy jointed rocks). |
| GB3 | Water pressure; an important load to consider in design especially in heterogeneous rock conditions.<br>A) Groundwater initiated failures may cause flowing ground in particulate materials exposed to large quantities of water, and trigger unstable conditions (e.g. swelling, slaking, etc.) in some rocks containing special minerals. Water may also dissolve minerals like calcite in limestone.<br>B) Water may also influence block falls, as it may lower shear strength of unfavourable joint surfaces, especially those with soft filling or coating. |

### 3.4.1 Examples of possible fall of ground and blast damages in TASS

The Figures 3-6 to 3-11 depicts different types of possible fall of ground and blast damage observed in the TASS.

***Figure 3-6.*** *Example of a spot bolted potentially loos wedge in the tunnel roof (marked in the figure).*

***Figure 3-7.*** *Example of geometry deviation in the end of a blast round. Note the bolted block in the beginning of the next round.*

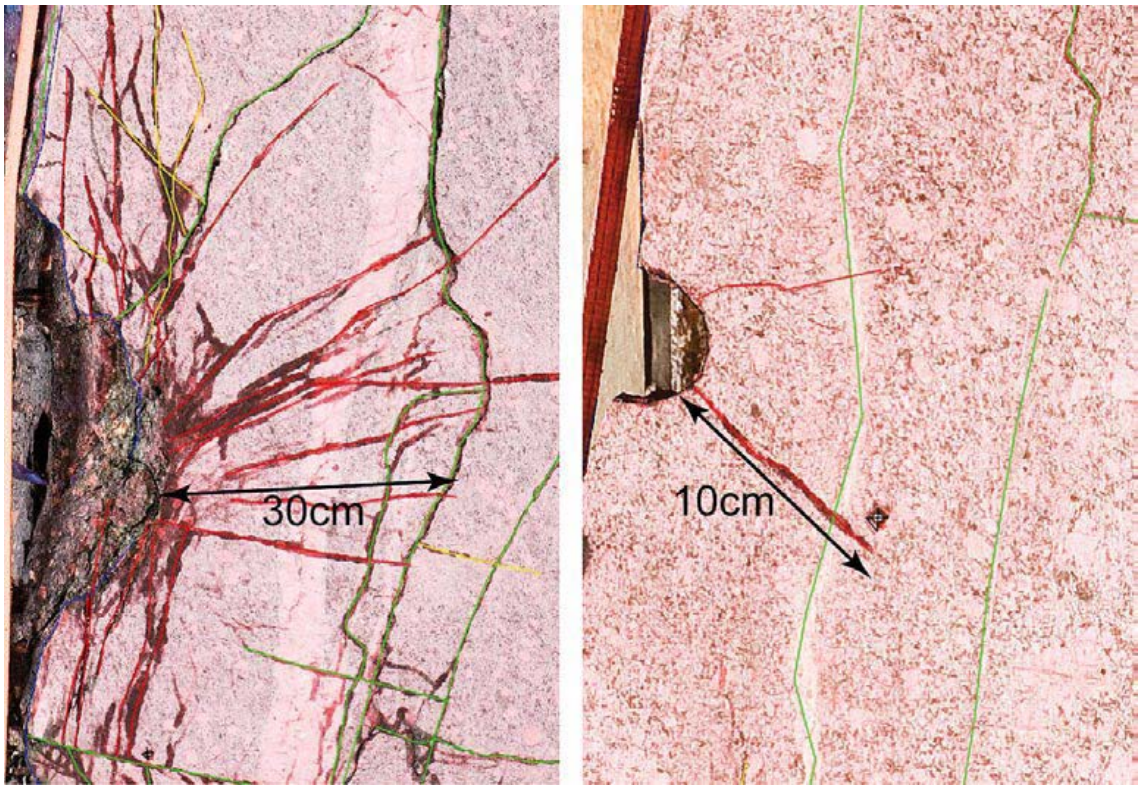


***Figure 3-8.*** *Left: An example of induced fractures in a blast hole bottom in the end of the blast round (bottom charge). Right: Blast hole bottom from column charge. Red lines indicate blast fractures and green lines natural fractures (Olsson et al. 2009).*

***Figure 3-9.*** *Overbreak in the area between two blast rounds. The area boundary is marked with yellow spray paint.*

***Figure 3-10.*** *Example of fall of ground in the last blast round of the TASS. The block is marked with a red circle in the figure. It originated close to a section supported with chain linked wire mesh.*

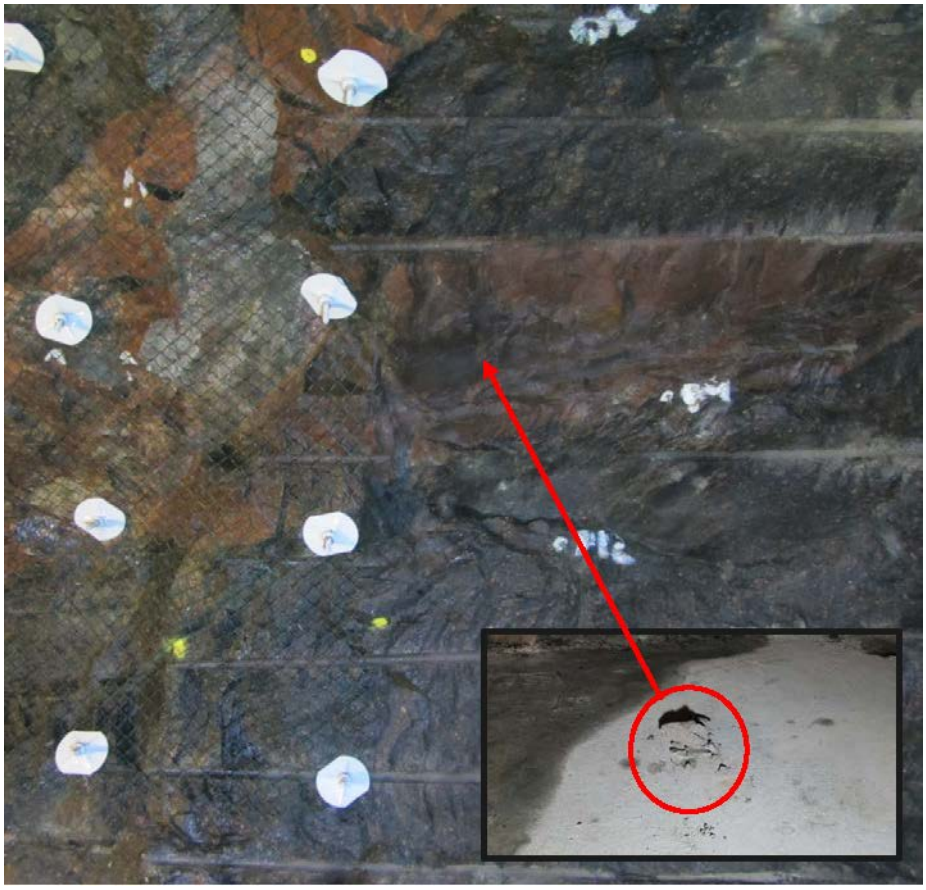

***Figure 3-11.*** *Roof of the section in Figure 3-10 with the fall of ground depicted to the lower right. The fall of ground originates from an area marked in the figure (outside the supporting wire mesh).*

# 4 Stability analysis

## 4.1 Simulation of induced stress

Ittner (2011) conducted stress simulations of 15 2D sections from the laser scanned TASS in Äspö HRL. The sections were located in the end of the blast rounds, were most maintenance scaling of loose blocks are performed. The magnitude of induced stress was plotted over the tunnel roof in order to identify stress peaks exceeding the crack- and spalling-initiation limits. The simulation was conducted with the finite element program Phase$^2$.

The same analyse method have been applied to Forsmark conditions by simulation of the TASS contour with Forsmark rock mass parameters and stress magnitudes. As the completed deposition tunnels have continuous geometry, the analysis can be simplified to a 2D in-plane case. Deviations from the 2D model could occur near the tunnel face or close to the intersection between the deposition and main tunnels.

The induced stress, due to excavation, is plotted together with the crack initiation strength, $\sigma_{ci}$, as it indicates a possible risk for spalling.

### 4.1.1 Theoretical section

The theoretical section of the TASS has been simulated with Forsmark rock mass properties (FFM01, see Table 2-6) and most likely stress magnitudes (Table 2-2), Figure 4-1.

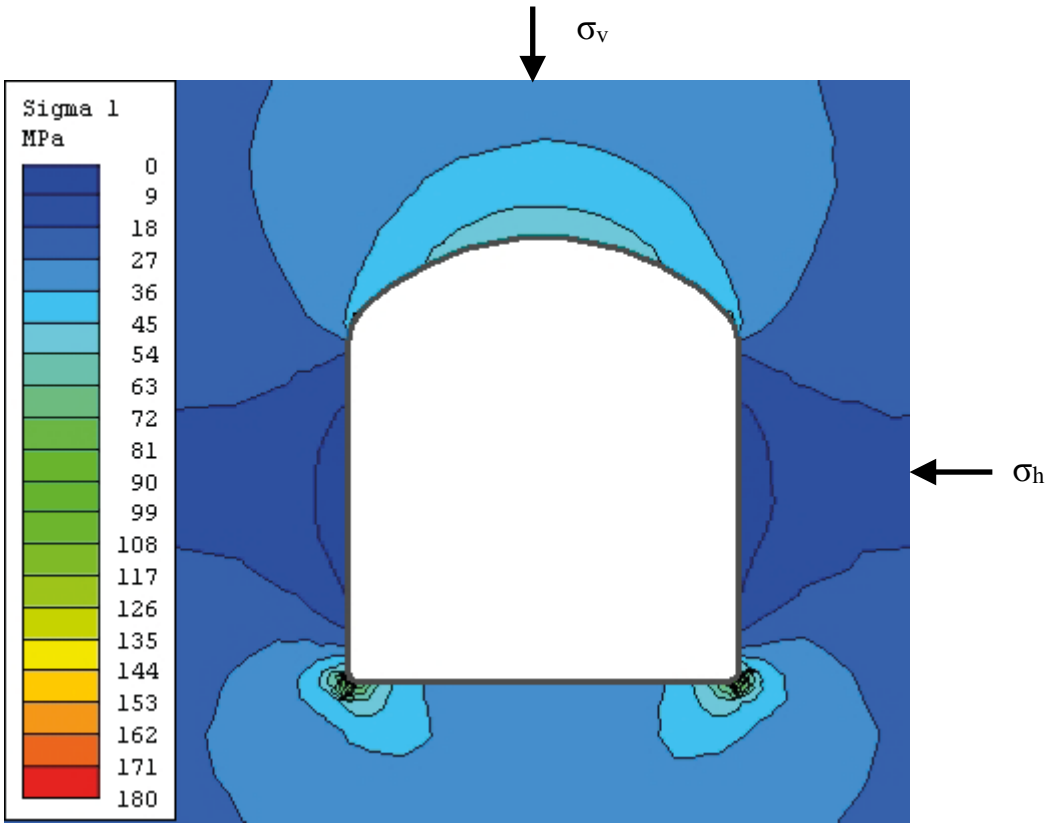


***Figure 4-1.*** *Most likely stress magnitudes of induced stress over the tunnel roof in the theoretical section of the TASS.*

The distribution of induced stress over the tunnel roof, together with limits for crack initiation, $\sigma_{ci,}$ for the most likely stress scenario is shown in Figure 4-2. The used values for crack initiation are for the rock type 101057, *Granite to granodiorite* in the rock domain RFM029, see Table 2-5. The crack initiation limit for the aplitic rock types in the area is higher.

For the worst case scenario, with maximum stress, the distribution of induced stress is presented in Figure 4-3.

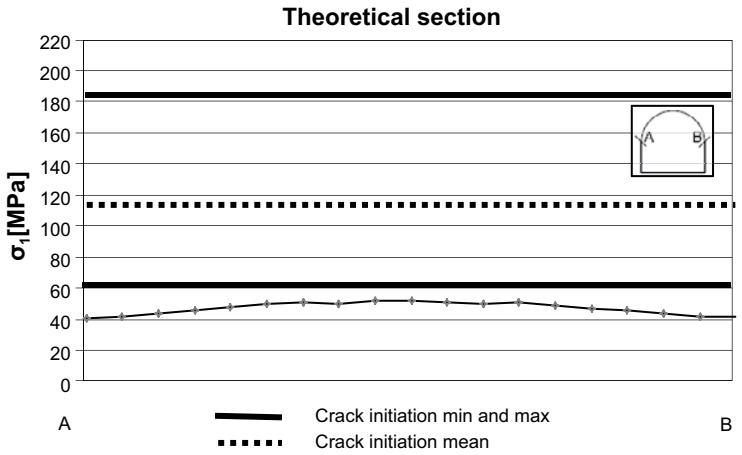


***Figure 4-2.*** *The distribution of induced stress over the tunnel roof, together with limits for crack initiation for the most likely stress situation.*

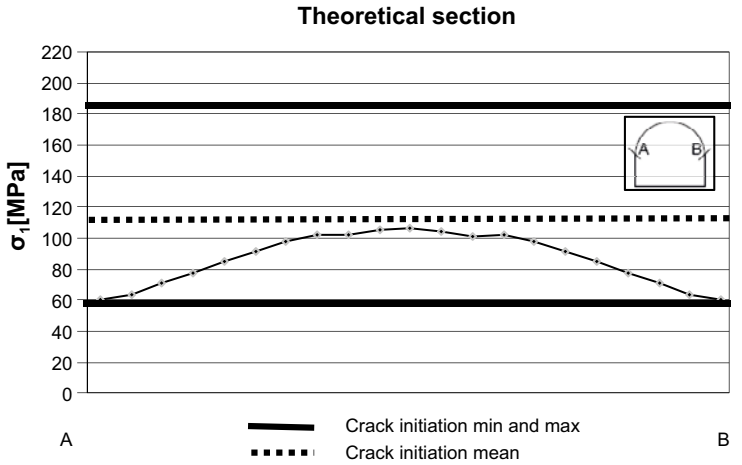


***Figure 4-3.*** *Worst case scenario with distribution of maximum induced stress.*

### 4.1.2 Sections from laser scanning

Sections from the laser scanned TASS have been used for this simulation. Two stress scenarios, the most likely and the worst-case scenario have been simulated using rock mass parameters for the fracture domain FFM01, Table 2-6. Figure 4-4 shows the most likely stress scenario (induced stress $\sigma_1$) in section 42 m.

Figure 4-5 shows the distribution of induced stress $\sigma_1$ in the tunnel roof in section 42 m.

Figure 4-6 shows the distribution of induced stress in the tunnel roof in section 42 m for the worst case scenario, $\sigma_{1\ max}$.

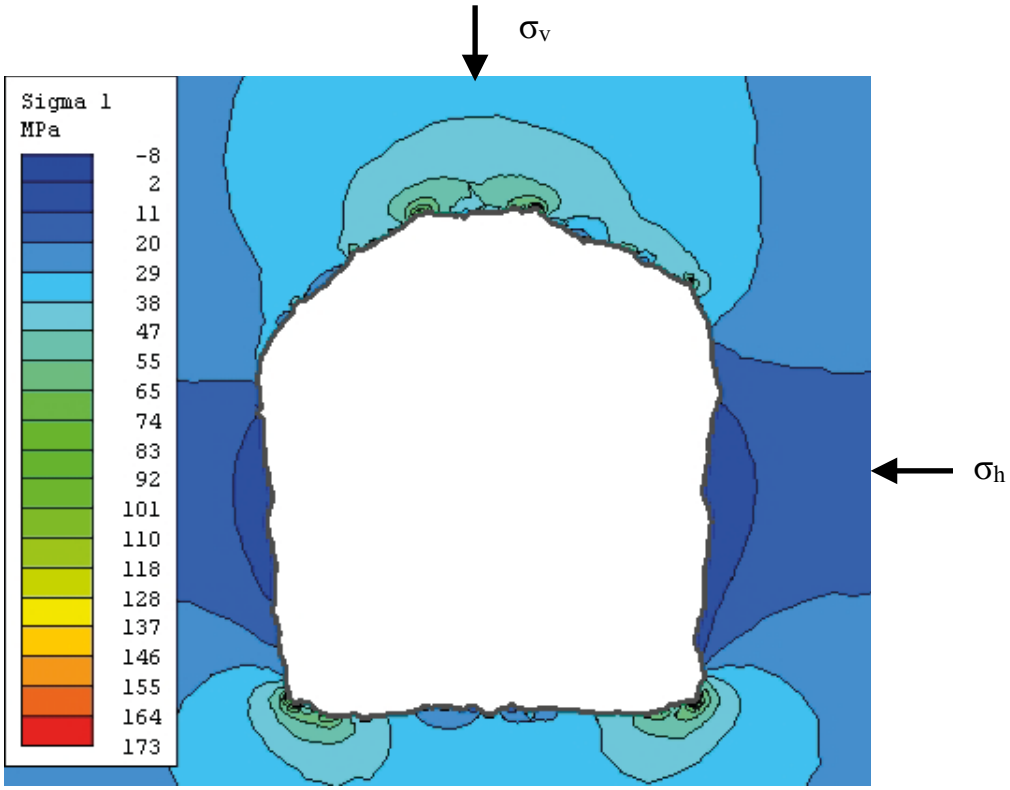


***Figure 4-4.*** *The most likely stress situation (induced stress $\sigma_1$) in section 42 m.*

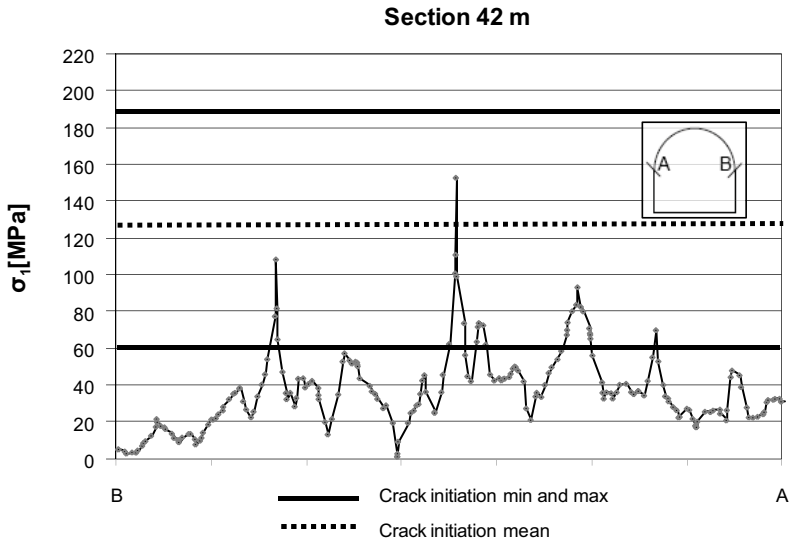


***Figure 4-5.*** *The distribution of induced stress $\sigma_1$ in the tunnel roof for the most likely scenario, section 42 m.*

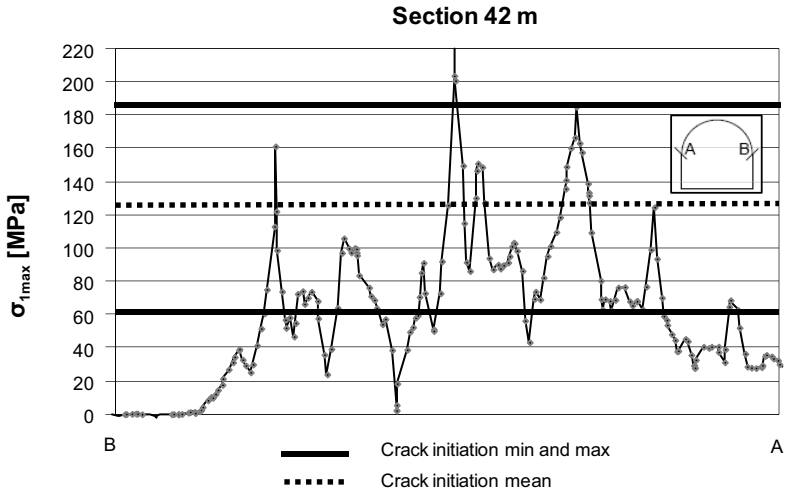


***Figure 4-6.*** *The distribution of induced stress in the tunnel roof in section 42 m for the worst case scenario, $\sigma_{1\ max}$.*

### 4.1.3 Interpretation of induced stress simulation results

The results presented in Figures 4-1 to 4-6 suggests stress induced spalling to be limited to relatively small overbreak areas in the tunnel roof. The effect could increase in sections with locally higher stress, as suggested in Figure 4-6. The walls are generally in a situation with low stress or tension, indicating a risk for gravity induced block falls. There may also be risk for gravity induced block falls in parts of the roof with low stress or tension.

Figure 4-7 and 4-8 shows the spots in the tunnel roof were the crack initiation minimum and mean are exceeded for the two simulated cases. As suggested by the figures cracks could propagate between over break areas in the roof.

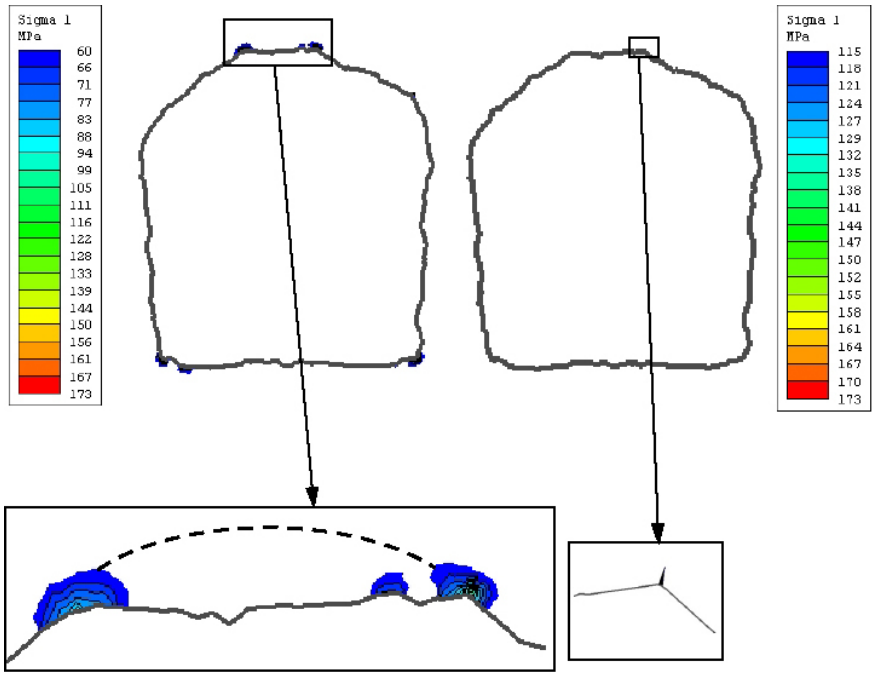


***Figure 4-7.*** *Noted in the figure are spots in the tunnel roof where the crack initiation minimum and mean are exceeded for the most likely stress situation. Upper left: areas were the minimum value of 60 MPa is exceeded. Upper right: areas were the mean value of 115 MPa is exceeded. Below: details of the contour, were the limits are exceeded. The dashed line indicates possible crack propagation between overbreak areas in the roof.*

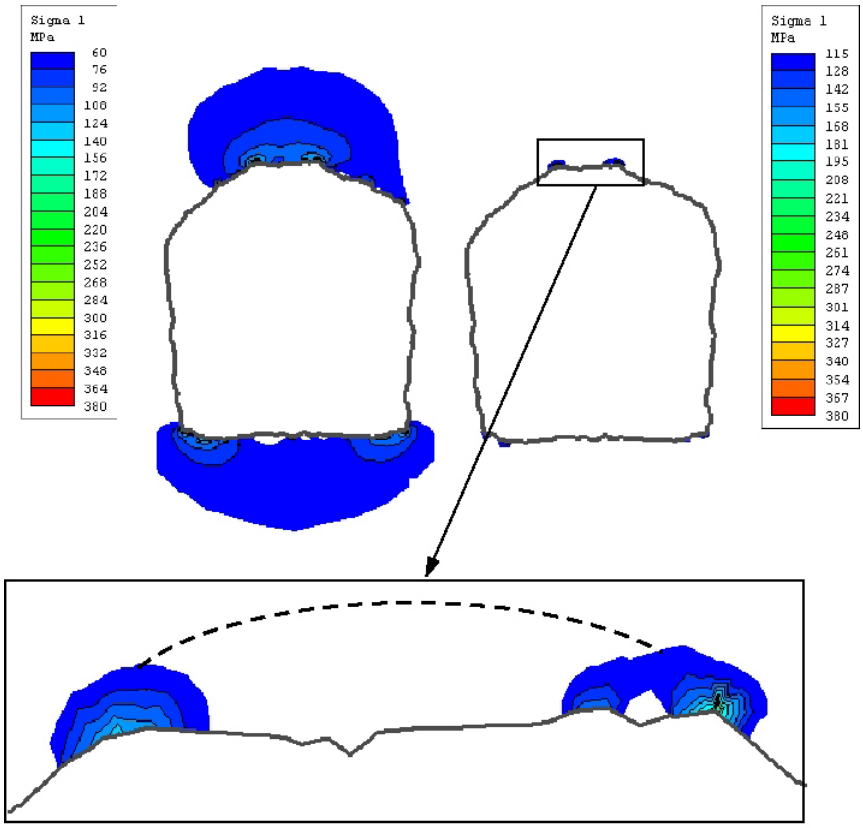


***Figure 4-8.*** *Noted in the figure are spots in the tunnel roof, where the crack initiation minimum and mean are exceeded for the worst case stress situation. Upper left: areas were the minimum value of 60 MPa is exceeded. Upper right: areas where the mean value of 115 MPa is exceeded. Below: details of the contour were the limits are exceeded. The dashed line indicates possible crack propagation between overbreak areas in the roof*

## 4.2 Induced stress from thermal loads

The influence on maintenance scaling and spalling from increased temperature in the excavation has been discussed by Andersson and Söderhäll (2001). After the installation of a heat producing compressor in the niche NASA 3419B in Äspö HRL, a lot of smaller rock fragments had to be scaled from the roof in the niche. This suggests that work with heat producing machinery, especially the drilling of deposition holes, may affect the magnitude of induced stress around the excavation.

Numerical stress simulations has been conducted with the two-dimensional finite difference code FLAC version 7.00 (Itasca 2011). Simulations of in plain induced stress were conducted in the sections 42 m and 77 m of the TASS. The sections were based on coordinates from the laser scanning of TASS. Rock mass parameters and in situ stress data were based on Forsmark values. The simulation was conducted with $\Delta T = 5$ °C giving 17 °C on the excavation boundary. The assumption on temperature increase was based on a normal operation situation and no worst case scenario was evaluated for heat increase.

Close to the boundary, most of the stress increase is obtained early in the warming period. The level of in plane induced stress for elements in unfavourably locations can be found in Table 4-1.

The same analysis were conducted for the section 77 m and results were collected after 5.6 days of heating for both the most likely and the worst case stress scenario. The analysis was conducted for both concave and convex areas at the excavation boundary, were extreme values of induced stress could be expected. Mean values of absolute change in magnitude of induced stress from thermal load ($\Delta\sigma$) are found in Table 4-2.

**Table 4-1. The level of in plane induced stress for elements in unfavourably locations in section 42 m. Likely level of in situ stress.**

| Value in element (269, 364), See Figure 7 in Appendix 1 | Sigma 1 (max. in xy plane) MPa | Sigma 2 (min in xy plane MPa) | Sigma zz out-of-plane stress component. | Max. disp. during this step | Temperature at element centre [°C] |
|---|---|---|---|---|---|
| Initially (in situ) | 23 | 13 | 41 | – | (12 in whole model) |
| After excavation | 148 | 20 | 71 | 1.36 mm | (17 on boundary) |
| After 6.3 days of heating | 159 | 21 | 77 | 41 µm | |

**Table 4-2. Mean values, for all of absolute change in magnitude of induced stress from thermal load, Δσ, for the section 77 m.**

| In situ stress | Geometry of excavation boundary. | Mean $\Delta\sigma_1$ (max in xy plane) [MPa] | Mean $\Delta\sigma_2$ (min in xy plane) [MPa] |
|---|---|---|---|
| Most likely | Concave | 9 | 1.6 |
| | Convex | 2 | 0.2 |
| Max stress | Concave | 8.6 | 1.25 |
| | Convex | 0.2 | 2 |

The results for the most likely stress conditions are presented in Figure 4-9 and Figure 4-10. Results for the situation with maximum stress are presented in Figure 4-11 and Figure 4-12 for the section 77 m. For the model mesh and complete results including stress and deformation plots, see Appendix 1.

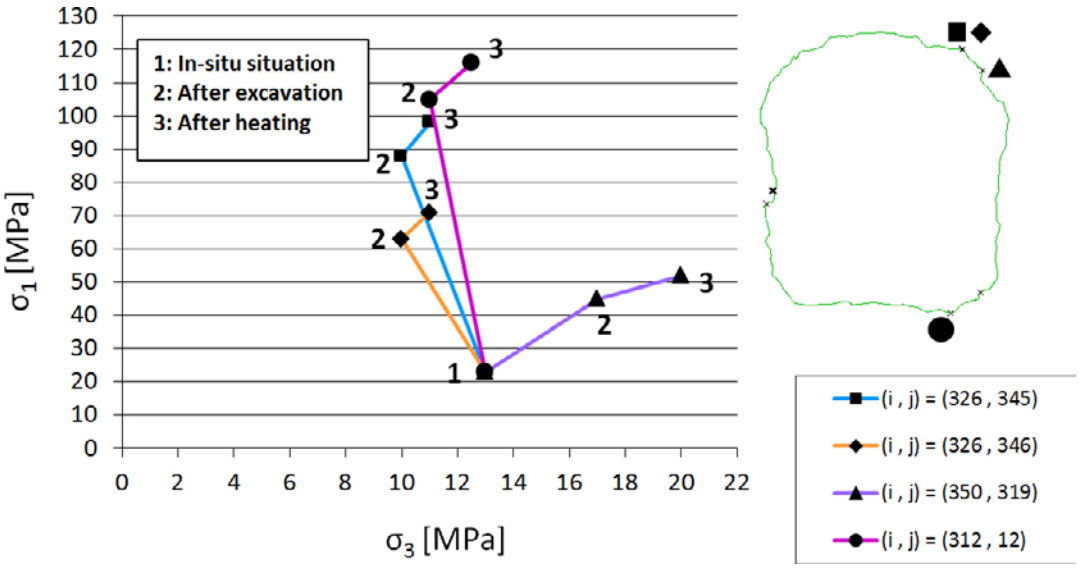


***Figure 4-9.*** *Stress path for elements in a concave part of the excavation boundary for the most likely in situ stress situation. Note that several elements are located close to another. The stress path contains three steps: in situ situation, after excavation and after 5.6 days of heating with 17 °C on the excavation boundary. Compare with crack initiation stress, Table 2-5.*

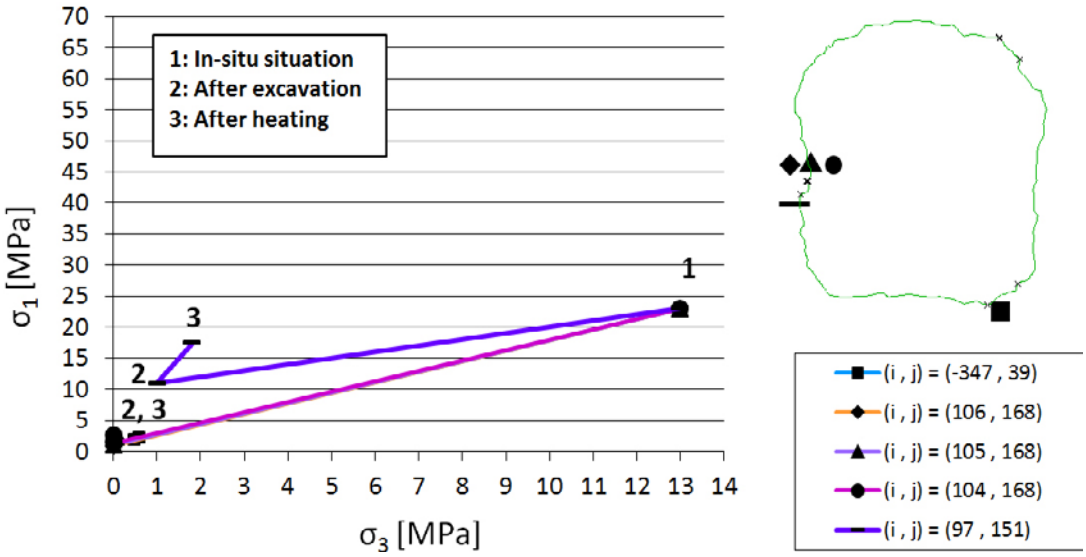


***Figure 4-10.*** *Stress path for elements in a convex part of the excavation boundary for the most likely in situ stress situation. Note that several elements are located close to another. The stress path contains three steps: in situ situation, after excavation and after 5.6 days of heating with 17 °C on the excavation boundary. Compare with crack initiation stress, Table 2-5.*

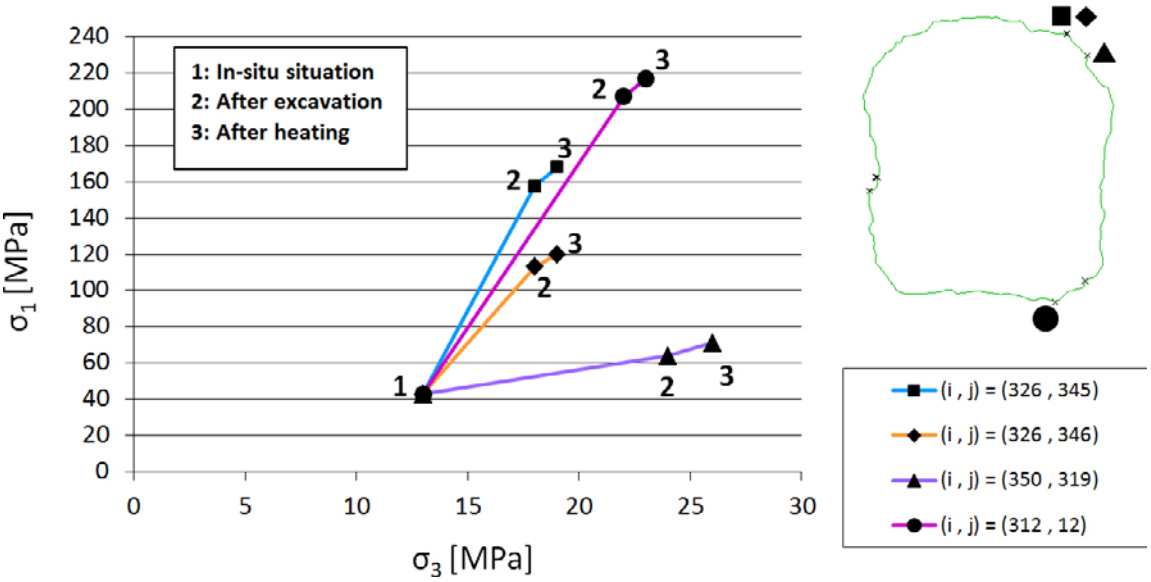


***Figure 4-11.*** *Stress path for elements in a concave part of the excavation boundary for the maximum in situ stress situation. Note that several elements are located close to another. The stress path contains three steps: in situ situation, after excavation and after 5.6 days of heating with 17 °C on the excavation boundary. Compare with crack initiation stress, Table 2-5.*

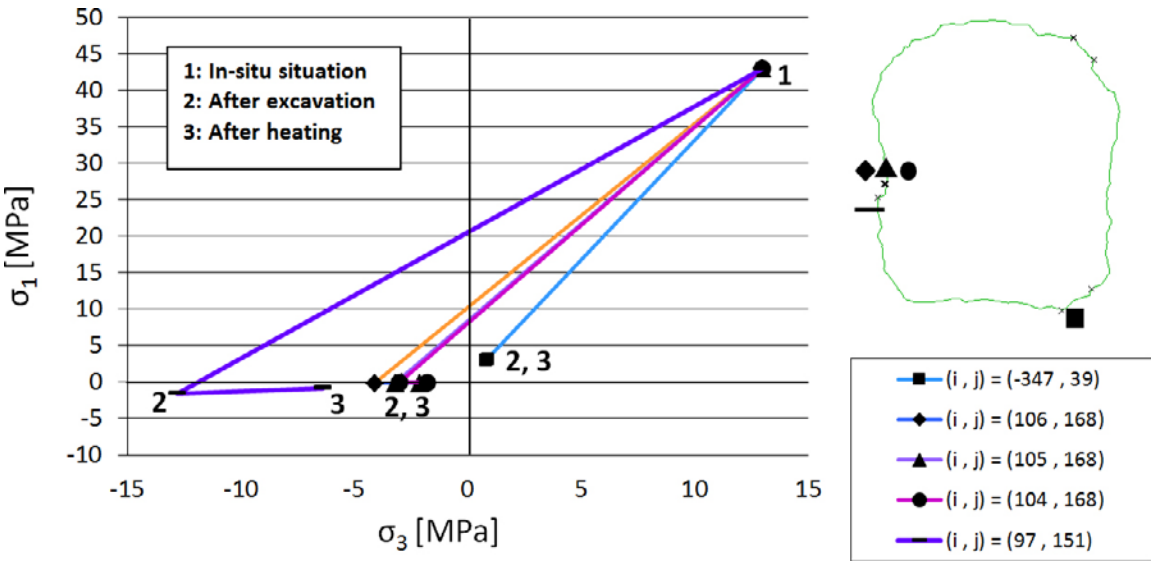


***Figure 4-12.*** *Stress path for elements in a convex part of the excavation boundary for the maximum in situ stress situation. Note that several elements are located close to another. The stress path contains three steps: in situ situation, after excavation and after 5.6 days of heating with 17 °C on the excavation boundary. Compare with crack initiation stress, Table 2-5.*

### 4.2.1 Interpretation of results from simulation of Induced stress from thermal loads

The simulation of thermal loads suggests that an increase in temperature in the excavation of 5 °C might, depending on the in situ stress situation, result in a change in magnitude of induced stress of approx. ± 10 MPa. If the rock mass is stressed near the crack initiation limit (See Table 2-5), the increased stress magnitude may result in brittle failure and possibly fall of ground.

Sections with low stress or tension, for example in the walls could be more stable at these levels of heating.

## 4.3 Gravity induced brittle failure

Deviations in geometry in the transition zone between two blast rounds can be unfavourable, also in sparsely fractured rock, for the stability of individual blocks. Induced stress is likely to be low and a block in this part of the tunnel roof is not locked in the direction opposite the tunnel heading, Figure 4-13.

***Figure 4-13.*** *Deviation in geometry in the end section of a blast round. Note the block supported with a rock bolt.*

In the case with sub-horizontal, natural or blast induced, fractures in this part of the tunnel a failure scenario can occur as proposed in Figure 4-14.

In order to analyze the reinforcement need for this type of brittle failure a simplification of the load case is made, Figure 4-15. The load case is simplified to a cantilever beam, loaded with its own weight and a loos block represented by a point load at the free end. This represents a more conservative case compared to a distributed load and simplifies the calculation.

The cantilever beam is calculated for plane bending, eq. 5-1, where the moment of inertia is given by $I = (H \cdot B^3)/12$ and $z$ gives the point in which the load from the beams own mass is applied.

$$\sigma = \frac{M}{I} \cdot z \qquad 5\text{-}1$$

Table 4-3 presents the maximum stress in the cantilever beam for different geometries. The tensile strength of the rock is assumed to be 8 MPa. The block loading the cantilever beam is based on the mean value from calculated blocks in Ittner (2009), 182 kg.

**Table 4-3. Maximum stress $\sigma_{max}$ for different geometries of the beam. The factor of safety is calculated with 2.4 MPa tensile strength of the rock mass.**

| Geometry | H [m] | B [m] | L [m] | $\sigma_{max}$ [MPa] | Factor of safety |
|---|---|---|---|---|---|
| 1 | 0.15 | 2.0 | 0.5 | 0.39 | 6.1 |
| 2 | 0.15 | 1.5 | 1.0 | 0.86 | 2.8 |
| 3 | 0.15 | 1.0 | 1.5 | 1.54 | 1.6 |
| 4 | 0.15 | 0.6 | 1.8 | 2.43 | 1.0 |

As expected, the case with a shorter but wider beam is more stable compared to a longer and slimmer one.

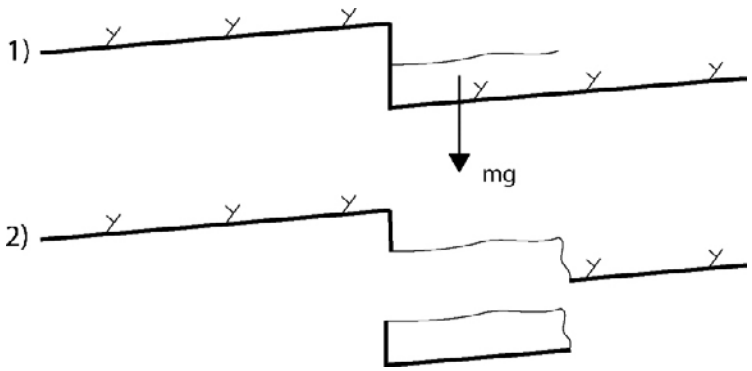


***Figure 4-14.*** *Schematic figure showing a possible failure scenario in the transition zone between two blast rounds. 1) The tunnel is excavated with deviation in geometry near a sub-horizontal fracture plane. 2) A brittle fracture propagates through the rock driven by stress induced from its mass and a block fall occurs.*

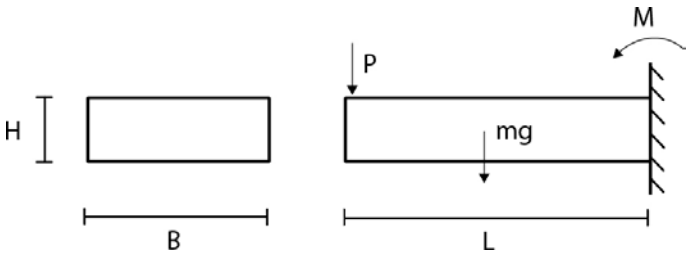


***Figure 4-15.*** *Load case where the block is simplified to a fix-end cantilever beam, loaded with its own weight. P is the point load from an additional loose block loading the beam.*

# 5 Rock support options

## 5.1 Strategy

Two major aspects are addressed during the design phase of underground structures. The first aspect is to determine the expected rock mass conditions and the resulting potential behaviour. The second aspect is design excavation and support according to the determined rock mass behaviour. A general procedure for the design of underground constructions is outlined by Goricki (2003), Figure 5-1. The procedure clearly distinguishes rock mass descriptions, behaviour of the rock mass as a result of the excavation and the behaviour of the whole system with both excavation and installed rock support.

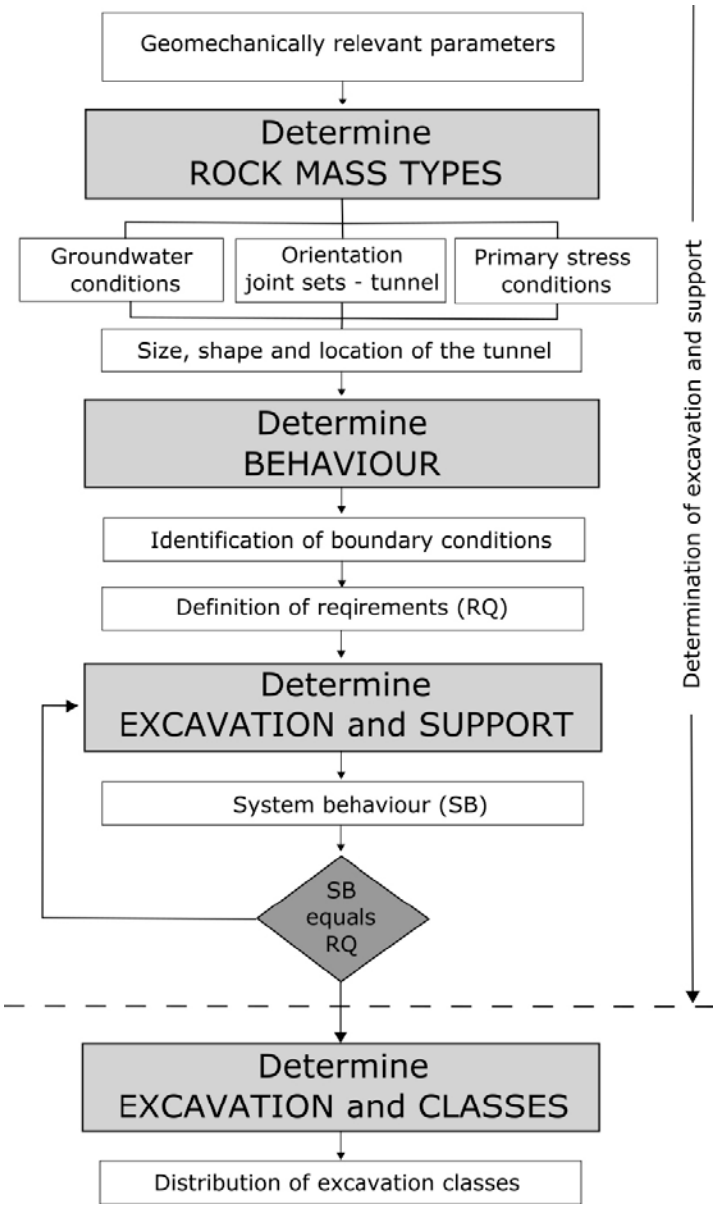


***Figure 5-1****. Process of excavation and support design for underground structures. Modified from Goricki (2003).*

## 5.2 Requirements

As the rock reinforcement methods for the excavation works shall be based on well-established, tried and tested techniques (SKB 2007**)** the proposed reinforcement alternatives for the deposition tunnels are rock bolts, shotcrete and wire mesh in combination with maintenance scaling. If otherwise equal approaches are discussed, the approach giving the lowest material use should be favoured. Technical working life of the deposition tunnels is 5 years minimum (SKB 2007).

Chapter 4 in SKB (2007) describes design requirements for the reinforcement system.

- Repository depth should take account of the risk of spalling.
- Orientation should be optimised with respect to the risk of spalling and geological factors (fractures and fracture zones).

The design and reinforcement of the repository has been optimised with regard to the rock mechanics of the area. The critical factors are occurrence and orientation of fractures and deformation zones, as well as any risks of stress-induced spalling. This was considered when orientation of the deposition tunnels was decided based on the in situ stress and fracturing.

Material used for rock reinforcement should not create unfavourable chemical conditions, which may affect the barrier function of the repository. All cement based material used in the repository must therefore have a pH < 11 according to a recipe given in Bodén and Pettersson (2011). In addition, cement based materials should only be used in a limited extent as they may disturb the function of the bentonite backfill and eventually form a continuous flow path along the tunnel once the concrete has degraded. This suggests an approach were shotcrete is used only in sections were the need for reinforcement is necessary for the safety of working personnel according to AFS 2010:1 (Arbetsmiljöverket 2010).

## 5.3 Maintenance scaling

The alternative to installation of a permanent rock support system is to conduct maintenance scaling of free rock surfaces on a regular basis. During scaling it is important that the workspace is well lit and free from disturbing noise (Arbetsmiljöverket 2010. The praxis at the Äspö HRL is to conduct regular maintenance scaling by hand from a work platform. Several alternative technologies are available including mechanical scaling (punching or tearing) and water-jet scaling. Figure 5-2 shows maintenance scaling conducted by hand in TASS.

***Figure 5-2.*** *Hand scaling in TASS.*

## 5.4 Rock bolts

A rock bolt is used for stabilizing rock excavations, such as tunnels or slopes. It transfers load from the unstable exterior, to the confined (and much stronger) interior of the rock mass. Rock bolts work by joining the rock mass together sufficiently before it can move enough to loosen and fail by unravelling (piece by piece). Rock bolts can be used either systematic or as spot bolts to secure single unstable blocks. Rock bolts can become 'seized' throughout their length by small shears in the rock mass, so they are not fully dependent on their pull-out strength. It is however the best use of the tension strength of a bolt to place it so the risk for shearing is minimized. Bolting pattern is therefore many times adjusted to the geological situation, Figure 5-3.

The arising deformations and stresses around an excavation in rock are a result from the interaction between rock mass and rock support. Analytical solution can be achieved under certain conditions. A general process for rock bolt support design with analytical method is given in Trafikverket (2014), Figure 5-4.

In the deposition tunnels grouted rock bolts or friction bolts will be used to secure larger blocks. This enables an approach were shotcrete and wire mesh can be more adequately designed. Rock bolts may be used to support wire mesh, but this is usually a small part of their function.

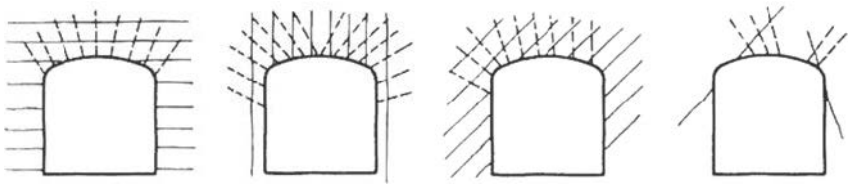

***Figure 5-3.*** *Different systematic bolt patterns, adjusted to the structure of the rock mass and selective bolting (far right).*

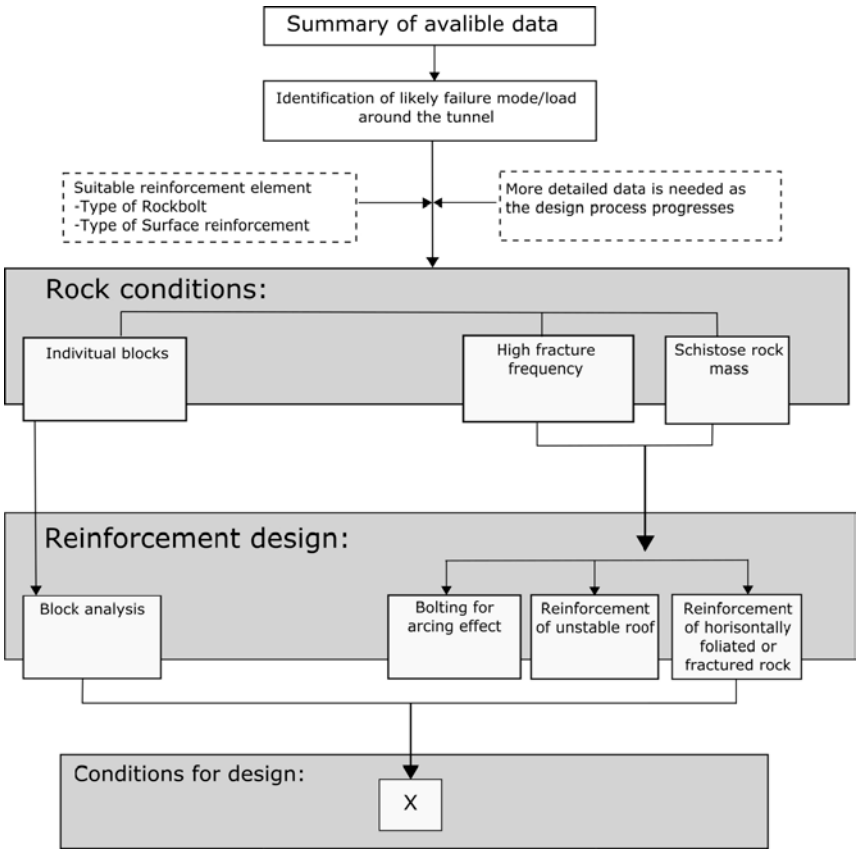


***Figure 5-4.*** *General process for rock bolt support design with analytical methods (Trafikverket 2014).*

## 5.5 Shotcrete

In hard rock tunnelling a shotcrete lining has the main function to stabilize potentially rotating or sliding key blocks. Stresses will however be induced and distributed into the shotcrete by small movements in the rock mass until a state of equilibrium has been reached (Holmgren 1979). This requires that further loosening of key blocks can be avoided.

A loose block punching through the shotcrete lining will occur after the initial elastic state lead to adhesion cracking in the contact surface between shotcrete and rock. Continued loading will then cause flexural or shear cracking, Figure 5-5. According to Holmgren (1979) adhesion cracking is independent of the layer thickness of the shotcrete in the range 20 to 80 mm.

A punch loaded shotcrete arc will induce a normal stress parallel to the contact area between rock and shotcrete. If the arc is unsupported an adhesion crack can propagate along the arc. Figure 5-6 shows sketches of supported and unsupported shotcrete arcs. In order to take advantage of a shotcrete arc, it is important that the shotcrete is applied to and supported by the abutment or floor of the tunnel (Holmgren 1979).

A general process for shotcrete support design with analytical method is given in Trafikverket (2014), Figure 5-7.

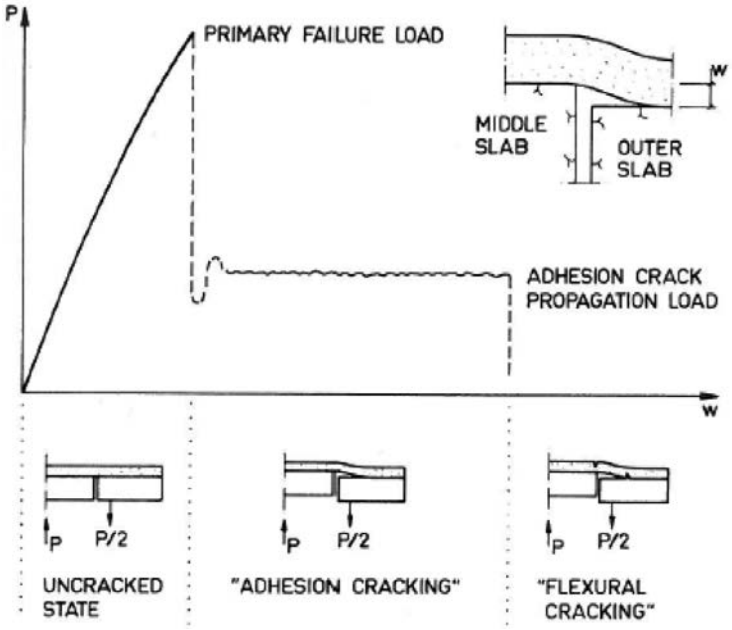


***Figure 5-5.*** *Failure modes with continued punch loading of a shotcrete layer (Holmgren 1979).*

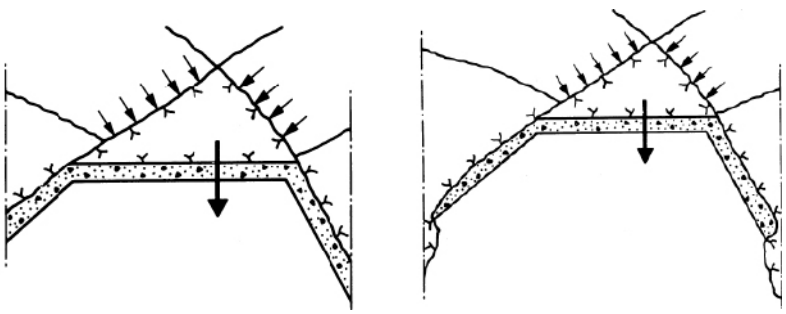

***Figure 5-6.*** *Sketches of supported and unsupported shotcrete arcs. Modified from Holmgren (1979).*

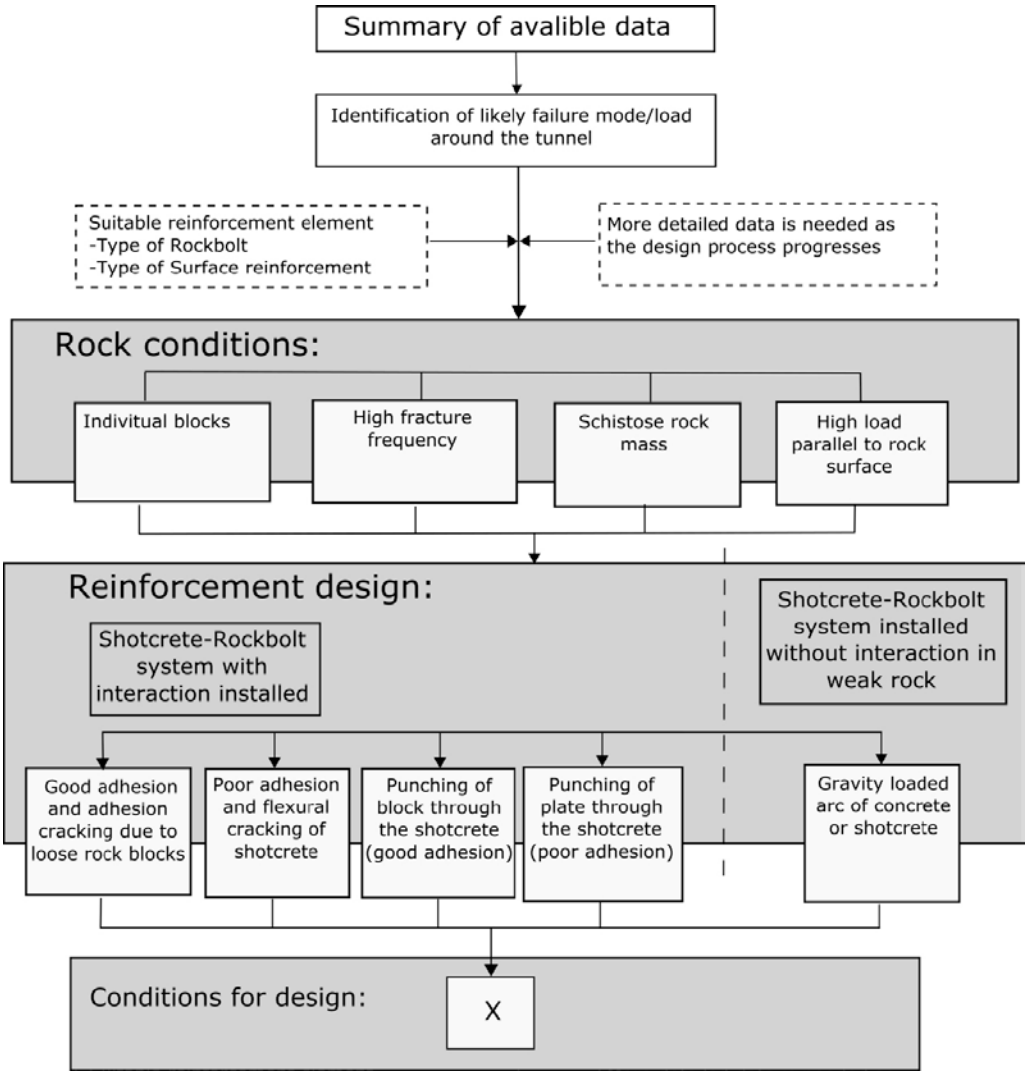


***Figure 5-7.*** *General process for shotcrete support design with analytical methods (Trafikverket 2014).*

## 5.6 Wire mesh

Hoek et al. (2000) describes wire mesh types and applications. Two types of steel wire mesh is commonly used, chain linked and welded. Chain linked mesh is more ductile and easier to apply to a rough rock surface but if the surface is reasonable smooth and there is enough room to work a welded mesh is the better choice. Figure 5-8 shows chain linked and welded wire mesh together with rock bolts who keep them in place.

Wire mesh has the advantage that the rock surface is assessable to inspection, mapping and other activities. It is also relatively easy to remove. A serious problem with wire mesh is corrosion. To avoid this, the mesh can either be galvanized or made of stainless steel.

Chain linked wire mesh is available with different types of braiding. For rock support purposes it is better to use a more complex braided mesh, as the failure of a single wire can propagate if the mesh is single braided. Figure 5-9 shows installation of double braided wire mesh in TASJ, Äspö HRL.

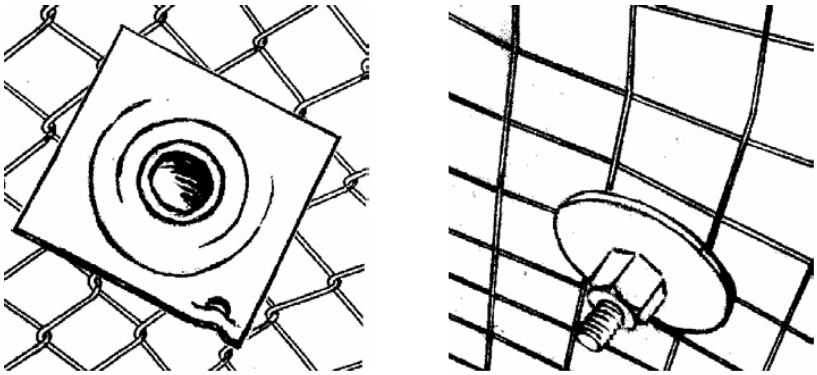

***Figure 5-8.*** *Chain linked, single braided wire mesh, left, and welded wire mesh, right (Hoek et al. 2000).*

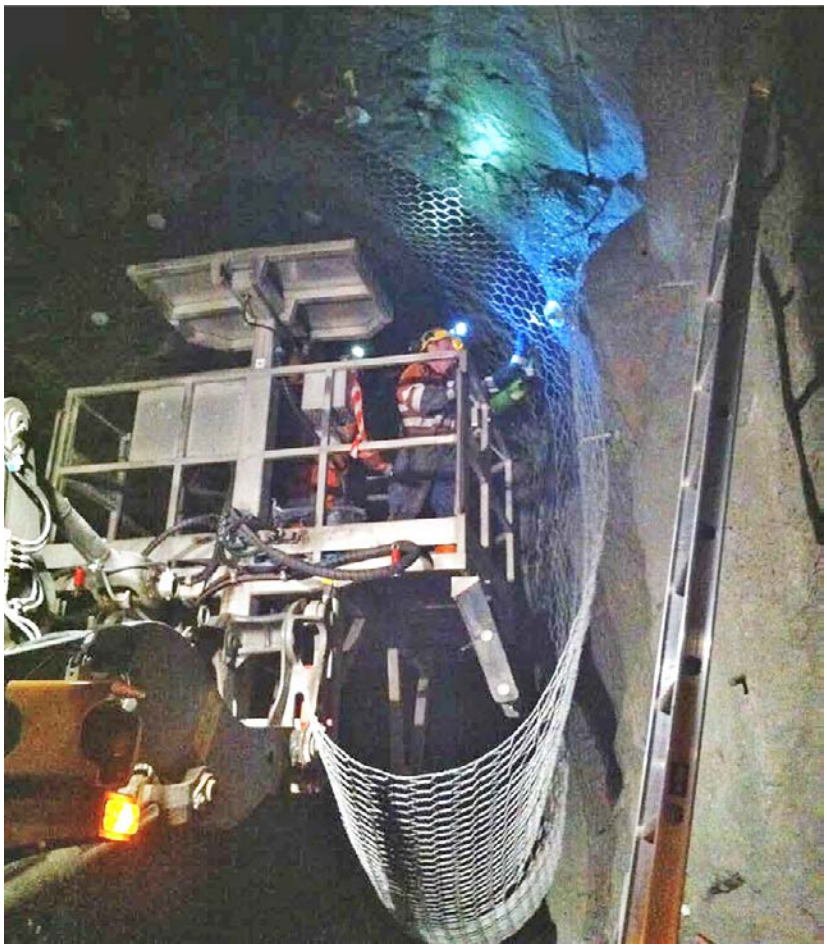

***Figure 5-9.*** *Installation of double braided wire mesh in TASJ, Äspö HRL.*

# 6 Experience of rock support in Äspö HRL

## 6.1 Rock support in TASA access ramp

The design work of the Äspö HRL started in 1989 and the tunnels were excavated during the period 1990 to 1995. The blasting works were conducted with a flexible approach from the start, allowing adjustments to be made as knowledge increased about the rock mass conditions once the excavation work proceeded (Carlsson and Christiansson 2007). Ordinary tunnel support and grouting technology was used during construction. However in order to be able go back and study exposed rock surfaces and hydrogeology, shotcrete, wire mesh, rock bolts and grouting was preformed to a limited extent. The facility has been subjected to regular maintenance scaling during the operative phase.

### 6.1.1 Maintenance scaling in TASA access ramp

Ittner (2009) conducted mapping of scaled areas in the tunnel roof of the TASA access ramp of the Äspö HRL. Five different area types were identified and their size and locations were noted. Based on this a method to evaluate the results from the mapping together with scaling records was developed. One of the conclusions from this survey was that over 50 % of the scaled areas were located in and caused by blast hole bottoms near the end of the blasting rounds. Those areas were generally small compared to the other types. Figure 6-1 shows the distribution of different causes for loose blocks scaled down from the tunnel roof.

## 6.2 Maintenance scaling and rock support in TASS

### 6.2.1 Maintenance scaling in TASS

The TASS has been subjected to maintenance scaling on a regular basis. During scaling occasions the mass of scaled rock material has been noted for each blasting round. It has also been noted were the scaling was conducted, i.e. right wall, left wall, roof or abutment. Figure 6-2 shows the mass of rock in each blasting round, scaled in the roof and abutment during the period august 2009 to June 2010. Note that the scaling is compiled for the whole section and not only for the blast round end.

Maintenance scaling has been conducted with longer intervals in the tunnel after the period noted in Figure 6-2. Scaled volumes are however only noted at two occasions and not for individual sections.

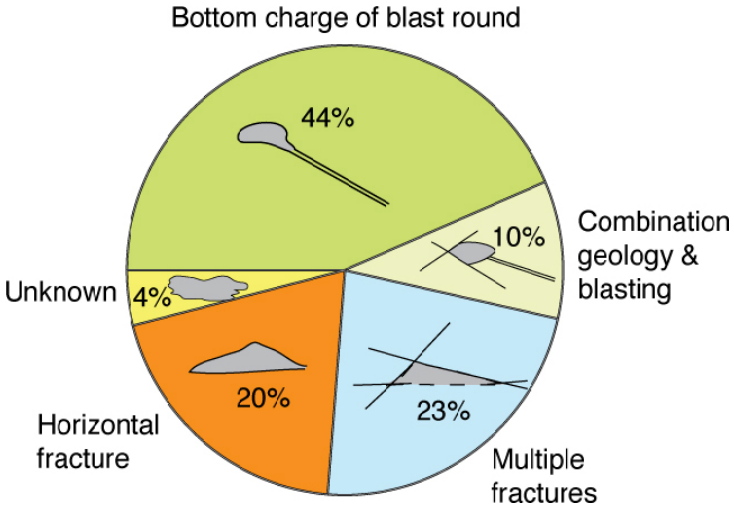


***Figure 6-1.*** *The distribution of different causes for loose blocks scaled down from the tunnel roof in the TASA access ramp. Modified from Ittner (2009).*

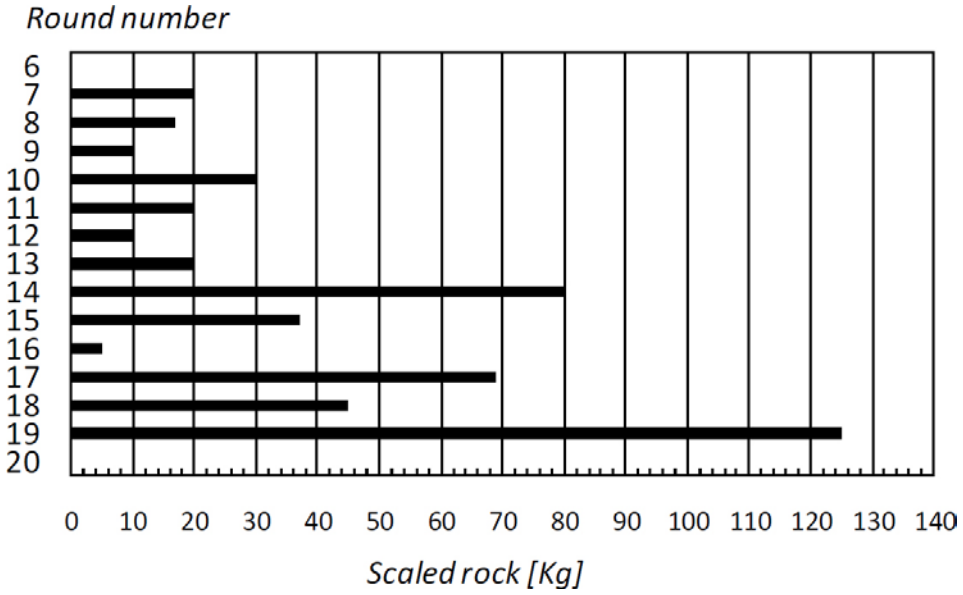


***Figure 6-2.*** *Total weight of scaled material from the roof and abutment for each round during the period august 2009 to June 2010. Data from maintenance scaling (Ittner 2011).*

### 6.2.2 Mapping as basis for support design

During spring 2011 selective shotcrete and wire mesh was applied in TASS in Äspö HRL based on inspection and mapping of the tunnel conducted in February 2011. The mapping was the basis for support design. The support solutions available were shotcrete and wire mesh combined with continued maintenance scaling. The following features were noted during the mapping:

- Deviation from theoretical tunnel contour in the transition area between two blasting rounds.
- Intersecting fractures, forming wedges.
- Maintenance scaling due to blast damage.
- Rock loosened by blast damage in otherwise undisturbed rock mass.

In addition mapping of scaled blocks with a combination of blast damage and geology were conducted. The mapping was the basis for recommendations of rock support for each blast round end.

Separate from the mapping a theoretical evaluation of the reinforcement need was conducted by Ittner (2011). The theoretical evaluation verified the results from the mapping, with a larger need for a surface rock support in the start and end of the studied parts of the tunnel. The evaluation was based on numerical stress simulation of 15 2D sections from the laser scanning of the TASS, fracture statistics and practical experience. The recommendations from the mapping and the theoretical evaluation are presented in Table 6-1.

**Table 6-1. Results from the mapping and theoretical evaluation. The suggested rock support for each of the section is noted with a color. Green for maintenance scaling, yellow for wire mesh and grey for shotcrete. Modified from Ittner (2011).**

| Section [M] | 24.7 | 28.8 | 32.8 | 37.3 | 42 | 45.6 | 48.5 | 52.6 | 56.6 | 60.4 | 64.4 | 68.7 | 73 | 77 | 80.5 |
|---|---|---|---|---|---|---|---|---|---|---|---|---|---|---|---|
| Mapping | | | | | | | | | | | | | | | |
| Theoretical evaluation | | | | | | | | | | | | | | | |

### 6.2.3 Shotcrete

The aim of the works with selective shotcrete in TASS was to fill out overbreak areas, smoothen the contour and to create a shotcrete arc in the end of the most damaged blast rounds. Four sections were constructed, two of them in two layers, two sections with thickness 50 mm and two with thickness 100 mm. The maximum thickness was applied in the blast round end and then a decreasing thickness was applied in order to fill the overbreak areas.

The overbreak area boundary was marked with yellow spray paint before the works started and 50 and 100 mm markers were placed in the roof in order to ease the work for the operator and insure the desired thickness. The contractor used a shotcrete robot with one operator, one miner for assistance and one work supervisor. The shotcrete was wet mixed and transported to the work site from a local concrete factory. There were several production stops due to malfunction of the shotcrete robot. The effective production time was 4.5 min/m.

The results of the production of the shotcrete were satisfactory. It was possible to smoothen the contour and to fill the overbreak areas. It was also possible to gradually decrease the thickness of the layer. It might be possible to create an arching effect in the shotcrete in the filled overbreak areas if the shotcrete can be supported by the area boundary.

Rebounded shotcrete were weighted. For this purpose a nonwoven fabric, covering the tunnel floor, was used.

After the shotcrete works was finished a laser scanning of the tunnel was performed. By comparing an earlier laser scanning with the new one the volume, mass and rebound of applied shotcrete could be estimated for each section, Table 6-2. The areas in the table are those of the applied shotcrete.

**Table 6-2. Shotcrete area, volume, mass and rebound for each section. Modified from Ittner (2011).**

| Section [m] | Area [$m^2$] | Volume [$m^3$] | Mass [kg] | Rebound [%] |
|---|---|---|---|---|
| 34.5–45.5 | 38.68 | 1.32 | 2904 | 43 |
| 53.5–60 | 23.09 | 0.49 | 1078 | 20 |
| 62–67 | 18.74 | 0.52 | 1144 | – |

Figure 6-3 shows the sections with applied shotcrete in TASS, based on the two laser scannings conducted.

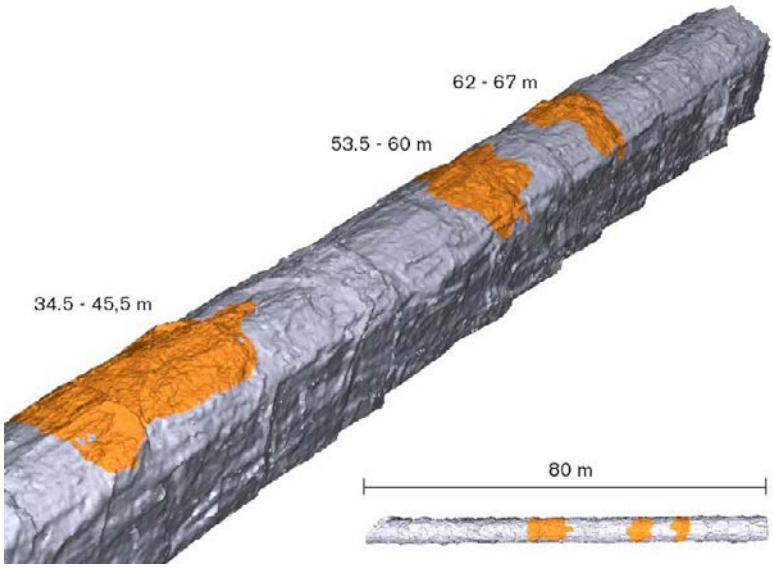


***Figure 6-3.*** *Sections with applied shotcrete, based on the two laser scannings. Shotcrete is marked orange in the figure. Figure by Pär Kinnbom (modified) (Ittner 2011).*

### 6.2.4 Chain linked wire mesh

Single braided chain linked wire mesh was installed in four selective sections of the TASS tunnel during May 2011. Gunnebo industrial fence was used together with 0.8 m grouted rock bolts. The bolt spacing was 0.8 m.

The installation of wire mesh was conducted by two miners in three stages:

1. Drilling of holes for the rock bolts.
2. Grouting of the holes and installation of rock bolts. The production steps were:

Mixing of grout, grouting of holes and installation of bolts.

3. Installation of wire mesh. The production steps were: Measuring and cutting of mesh and installation of mesh. Figure 6-4 shows the installation of wire mesh by hand.

Each of the stages required preparations before the activity could be carried out. Examples are mixing and testing of grout and measuring and cutting of wire mesh sections.

The results from the production of wire mesh are also satisfactory. The applied mesh, Gunnebo industrial fence (galvanized and covered with PVC-plastic), was easy to apply and has a good contact to the rock.

### 6.2.5 Method comparison

The contact between rock support and rock is better if shotcrete is used compared to wire mesh. This affect the ability of the support to stabilize small stress induced outfalls.

Ittner (2011) compared the production costs for the different support alternatives.

The result per meter suggests that the production cost per $m^2$ of shotcrete is approximately 20 % of the cost for wire mesh. This is however based on active production times. The actual production times include moving of the work platform or shotcrete robot and cleaning of workspace etc. Including those parts of the total production time would increase the costs for wire mesh more rapidly as more time consuming work steps are needed. For the shotcrete works the costs for shotcrete is most dominating and there are reasons to believe that costs could be lower in a large scale project. This supports the estimation that shotcrete is more cost effective then wire mesh.

***Figure 6-4.*** *Hand installation of chain linked wire mesh in TASS.*

# 7 Other reference methods for rock support

## 7.1 Dynamic reinforcement, LKAB mine in Kiruna

A concept of dynamic reinforcement is applied in LKABs iron ore mine in Kiruna. A welded wire mesh is applied to a fibre-reinforced shotcrete layer and secured with deformable rock bolts (D-Bolts), Figure 7-1.

The wire mesh is installed on the shotcrete layer in several steps depending on the method of application. In the Kiruna mine both installation by hand and mechanised installation are conducted. For the mechanized installation an Atlas Copco Boltec rig is used. The rig features two booms; one for drilling, injecting and bolt installation (swellex) and one for handling and holding wire mesh in place during installation. The rigs also feature an automatic cement handling system. Figure 7-2 and Figure 7-3 depicts the rig during installation of wire mesh.

Installation by hand is conducted in three steps. First the wire mesh sections are installed, with an overlap, and hand pressed to follow the shotcrete contour. The mesh is held in placed by a small fastener, drilled in place with a hand drill. Then holes for D-Bolts are drilled and grouted and the D-bolts are installed. Figure 7-4 shows the fastener, marked with a red circle in the figure.

The mesh is delivered in sections of 2 370 × 2 530 mm. The wires are 5.5 mm thick with aperture 75 mm. Figure 7-5 shows sections of the mesh temporary stored in the tunnel prior to installation.

***Figure 7-1.*** *Dynamic reinforcement in the Kiruna mine.*

***Figure 7-2.*** *Installation of welded wire mesh with an Atlas Copco Boltec rig.*

***Figure 7-3.*** *Installation of welded wire mesh with an Atlas Copco Boltec rig. The upper boom is holding the mesh with an electromagnet and the lower is installing a swellex rockbolt.*

***Figure 7-4.*** *Welded wire mesh, temporary holed in place with a hand drilled fastener, marked with a red circle in the figure.*

***Figure 7-5.*** *Sections of welded wire mesh.*

## 7.2 Rock support in the demonstration area in Onkalo

The demonstration area in Posivas underground characterization facility, Onkalo, consists of four shorter demonstration tunnels. The purpose with the demonstration tunnels is, as the name suggests, to demonstrate the technology of the KBS-3 concept in full scale. Demonstration tunnel 2 and 3 are both supported with an expanded metal-type of stainless steel mesh. During the excavation two rounds without support is accepted, after excavation of the third unsupported round, the stainless steel mesh is installed in the two previous rounds. The mesh is installed with systematic 3 m rock bolts, Figure 7-6 and Figure 7-7.

***Figure 7-6.*** *Stainless steel mesh and systematic bolting in Demonstration tunnel 3. The bolts are 3 m long.*

***Figure 7-7.*** *Detail of the stainless steel mesh (left) and drilling under reinforced roof (right). After excavation of the next round new mesh is to be installed.*

# 8 Discussion

## 8.1 Causes for fall of ground

The experience achieved during the work with rock support in Äspö HRL suggest that the parameters that influence the risk for falls of ground are natural and induced fractures and magnitude of induced stress. If the tunnel is excavated in an area with high density of natural fractures there is an increased risk for overbreak by non-conformities of the contour. Non-conformities of the contour will in turn affect the induced stress level and increase the risk for fall of ground due to spalling, Figure 8-1. The induced stress is in turn dependent on the in situ stress magnitude and changes in temperature in the excavation. The contour is also dependent on the quality of the blasting works, which in turn may reactivate sealed natural fractures.

The combined effect of the induced stress field around the tunnel face and a larger charge concentration in the bottom charge could explain the larger extent of excavation damage.

## 8.2 Support need in deposition tunnels

Main activities in preparing a deposition tunnel was summarized by SKB (2009b).

1. Rock construction works; 105 ± 10 weeks. This includes all construction and characterization of a deposition tunnel and the deposition holes.
2. Deposition works 32 ± 5 weeks. This includes all deposition and backfill activities and the completion of a plug close after the tunnel collar.

The reference method for construction is drill- and blast. The tunnel excavation can likely be carried out with one jumbo working at three to four faces at the same time. Drilling of deposition holes might likely require more than one machine; the drilling of deposition holes is likely going on in more than one tunnel at the time. Deposition and backfilling is going to be done in one tunnel at the time.

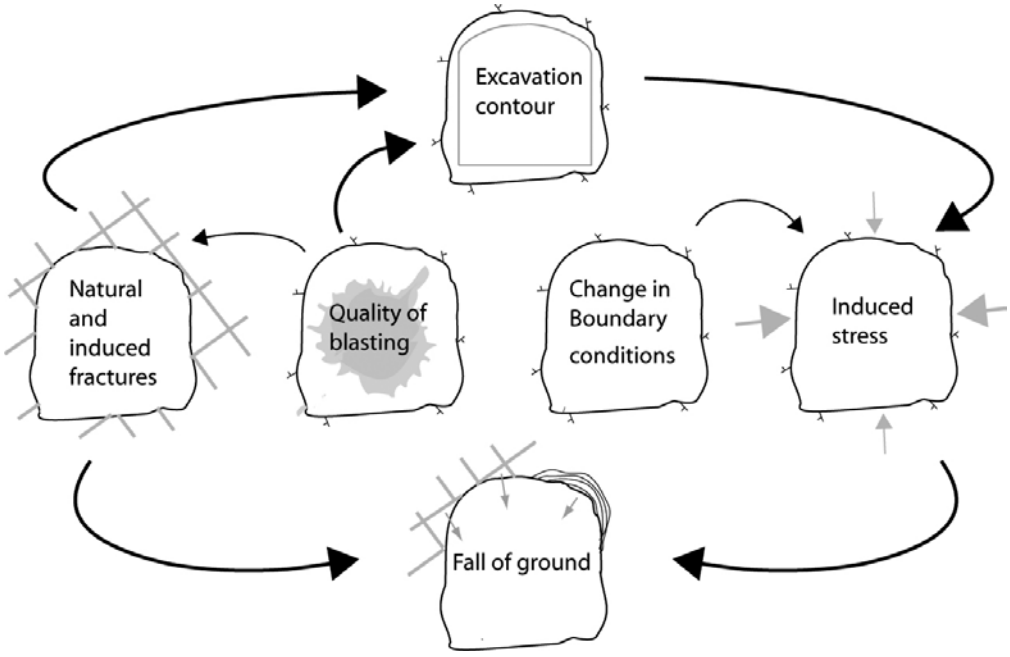


***Figure 8-1.*** *Influence between parameters controlling the risk for falls of ground. Natural fractures may cause overbreak during excavation and influence the contour. An unfavourable contour may in turn increase induced stress magnitudes around the excavation causing spalling. Intersecting natural fractures may also cause gravity induced falls of wedges.*

The estimated amount of rock support in SKB (2009a) is based on Eriksson et al. (2009). They concluded that for the actual deposition tunnel operational life time (ca 5 years) in good rock conditions with sparsely fractured, isotropic rock is loosening of local blocks the main concern. They estimated the need of support to be limited to in average a bolt every fourth meter in deposition tunnels. This does however not include the consequence of non-conformities in blast results and the rock support measures that have been experienced from the Äspö HRL (see Chapter 6). It must also be considered that the continuous excavation of deposition tunnels causes blast induced vibrations to nearby tunnels with a frequency much higher than in the Äspö HRL.

The state of stress approaches constant conditions at some point after construction. If the induced stress magnitude on the tunnel perimeter is below damage threshold, the only driving force to loosen up the rock surface is changes in boundary conditions such as the annual variation in temperature and humidity.

## 8.3 Results from stability analysis

The results from the stress simulation suggest that local cracking or spalling may occur in overstressed parts of the tunnel roof. The risk increases with local high induced stresses and cracks could propagate between over break areas in the roof. If the stress is near or lower than the most likely magnitudes of induced stress, the expected crack initiation and spalling is assumed to be limited. The walls are generally in a situation with low stress or tension, indicating a risk for gravity induced block falls. This suggests increased need for scaling of the walls. There may also be risk for gravity induced block falls in parts of the roof with low stress or tension.

The induced stresses are highest in the crown and overbreak in this part of the tunnel roof results in high concentrations of induced stress. If overbreak in the crown is combined with local high in situ stresses the induced stress is likely to exceed the crack initiation limit of the rock.

The results from the laser scanning of the TASS and stress simulation of tunnel section located near each other suggests that overbreak structures, resulting in high induced stresses, are frequently located in the end of the blast round and extended parallel to the tunnel.

The simulation of thermal loads suggests that an increase in temperature in the excavation of 5 °C might, depending on the in situ stress situation, result in a change in magnitude of induced stress of ± 10 MPa. If the rock mass is stressed near the crack initiation limit, the increased stress magnitude may result in brittle failure and possibly fall of ground.

## 8.4 Strategy for choosing rock support measures

The strategies and methods for choosing rock support methods in deposition tunnels are dealing with a number of decisions:

- To meet the overall requirement of a safe working place is the balance between inspections and maintenance scaling versus support measures to be found.
- The data base developed on scaling records at the Äspö HRL cover today up to 20 years of construction and operation. The strategies to utilize such a data base over scaling at repository level at Forsmark need to be developed in terms of data report format, evaluation frequency etc.
- The conclusion by Eriksson et al. (2009) that there is required very little rock support indicates the possibility that other rock support than selective spot bolting of blocks may be possible to minimize. There is also a cost aspect on the risk for over-use of support measures in the tunnels with short operational life time.
- The decision on final support shall be taken before it affects the planned deposition and backfill operations. Such decision is preferable based on documentation of scaling records.

## 8.5 Rock support alternatives

The most likely rock support of roof and abutments for the deposition tunnels are rock bolts, wire mesh and shotcrete based on a low-pH cementitious material combined with mechanical scaling.

Figure 8-2 presents a schematic overview of support alternatives for the blast round end.

Depending on the characteristics of a tunnel contour, especially at the blast round end, different support alternatives might be needed. In the end of a blast round all three failure types described in Section 3.4 could occur. If the different failure types could be recognized and separated an optimized support solution could be applied for the deposition tunnels.

Spalling problems are best handled with surface reinforcement, i.e. shotcrete or wire mesh. Larger blocks in the end of the blast rounds may need to be secured with rock bolts or scaled down through mechanized scaling. If however spalling problems and larger blocks occur in the same blast round, shotcrete reinforced with steel fibres could be applied. Larger wedges, referred to as type 2 in Section 3.4, will most likely require spot bolting.

An alternative to the solutions presented in Figure 8-2 is to use sheet or corrugated metal supported by steel arcs. This solution could be used to support sections or as a continuous support in the deposition tunnels. The support could be disassembled during backfill and reused as new tunnels are excavated. This method will eventually require that a larger tunnel section is excavated, if it is not possible to place the arcs in the overbreak at the blast round end.

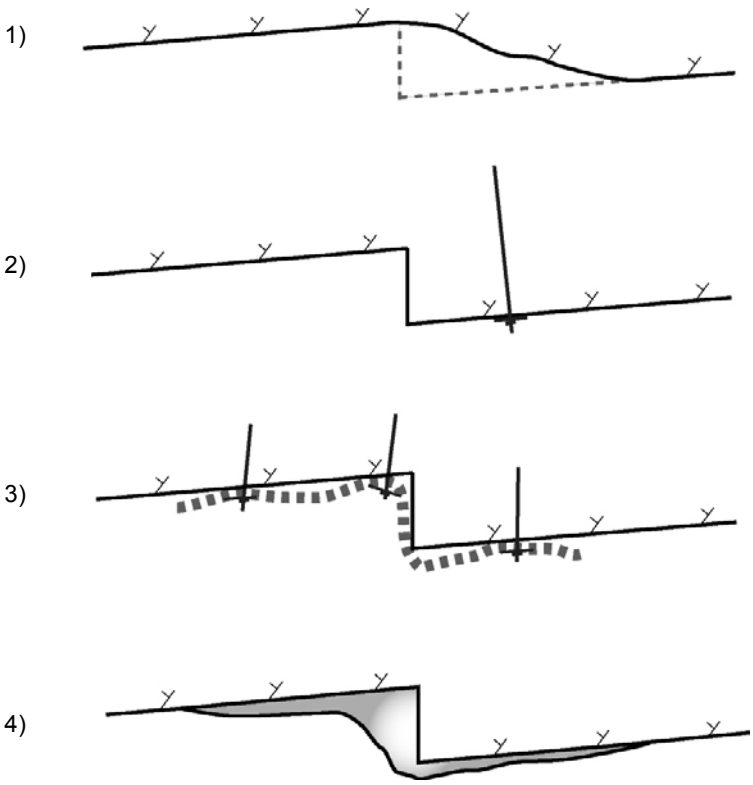


***Figure 8-2.*** *Schematic figures depicting the available rock support alternatives for the blast round end. 1) Mechanical scaling, 2) Rock bolt to secure block, 3) Wire mesh, 4) Selective shotcrete. Support alternatives 1 and 2 are better suited to handle problems related to block stability. Spalling or minor outbreaks are better controlled with a surface reinforcement of type 3 or 4.*

## 8.6 Influence from vibration

The need for maintenance by means of scaling of unsupported surfaces might need to be significantly higher in deposition tunnels, compared to current praxis at the Äspö HRL. Vibration data (primarily PPV) was compiled after the last to excavations campaigns at the Äspö HRL, the S-tunnel (Karlzén and Johansson 2010), and the Q tunnel (Nyberg et al. 2008). The results are summarized in Figure 8-3 and Figure 8-4 respectively. As shown in the figures the experience from two tunnelling projects within the Äspö HRL at 450-m depth is that it is unlikely that the maximum PPV exceed 10 mm/s at a distance of maximum 50 m. No damage related to blasting was found outside the construction areas of Q respectively S tunnels. However, this might be site-specific. The need for inspection frequency and scaling measures caused of blast damage during excavation of deposition tunnels for a repository at the Forsmark site has to be established based on systematic monitoring of vibrations and inspection procedures.

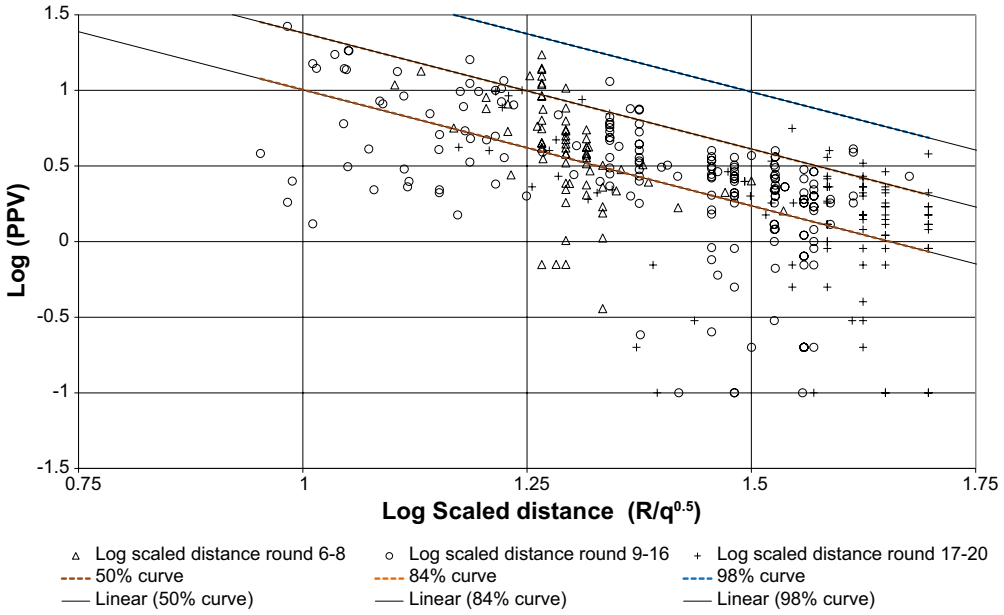


***Figure 8-3.*** *Log PPV (mm/s) as a function of Log scaled distance ($R/q^{0.5}$) for rounds 6-8 (Pyrotechnical initiation), rounds 9-20 (Pyrotechnical and electronic initiation) from TASS (Karlzén and Johansson 2010).*

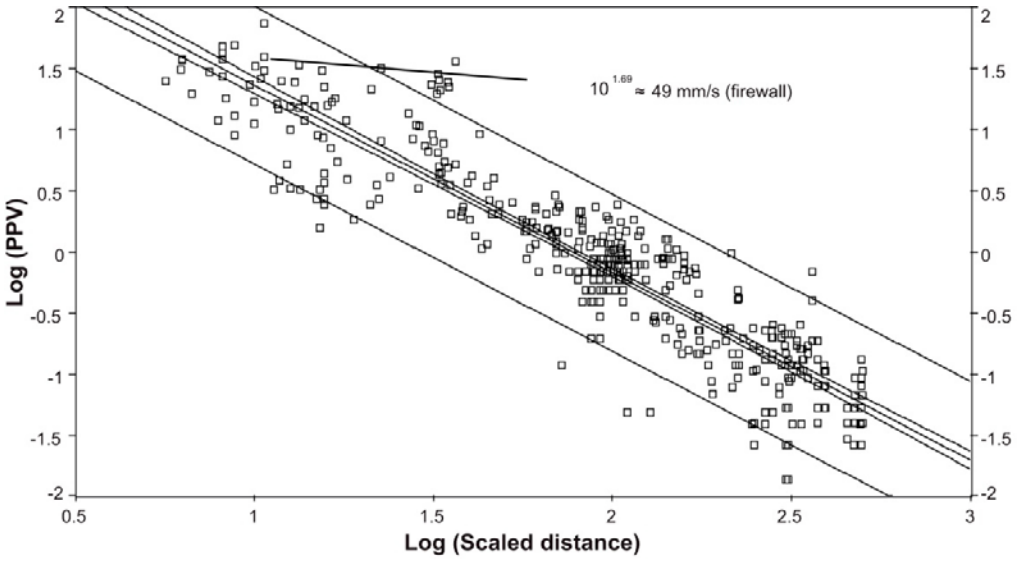


***Figure 8-4.*** *Log PPV (mm/s) as a function of Log scaled distance ($R/q^{0.5}$) for 419 top heading rounds data from the Q-tunnel (Nyberg et al. 2008).*

## 8.7 Preliminary risk assessment

The overall largest risks are serious damage to persons, as well as inconsequent decision processes that leads to incidents such as unexpected fall of ground in working areas. This can cause both fatalities, damage to equipment and lost confidence from the Regulator. The most effective mitigation of these risks is systematic support measures. As indicated by Eriksson et al. (2009) the need for rock support is limited to selective measures with spot bolts and wire mesh. A risk assessment according to the requirements stated in Arbetsmiljöverket (2010, §3) should however be performed. SKB need to establish a policy for rock reinforcement.

A systematic, conservative approach to rock support during or soon after construction provide a safe working environment in accordance to mining praxis. The negative consequence may be that a systematic characterization of the geological conditions might be affected. However, such issue has minor importance, because rock conditions require heavy support might not be suitable as deposition position. The cost for tentative over-use of support is marginal, but the consequence on workers safety and post closure safety has to be evaluated. The experience from Äspö HRL is that systematic scaling of tunnels in good rock conditions is sufficient to provide a safe working environment. The frequency of scaling has to be considered based on rock conditions and ongoing activities. It might also have to be considered that the lag time between main activities might vary. During such periods the tunnel ought to be closed for any entrance. The consequence of risk for fall of ground or disturbance on the activities is discussed in Table 8-1. A disturbance on the deposition and backfill activities is significant and must be avoided, even although systematic scaling might be sufficient to maintain workers safety. Systematic inspection and well documented scaling is a procedure that can contribute to sufficient, but not too much support to maintain a safe working place.

**Table 8-1. Consequence of risk for fall of ground or disturbance on activities.**

| Activity | Comment | Consequence |
|---|---|---|
| Tunnel excavation, support measures, drilling of pilot holes, grouting works and sawing of the tunnel floor. | The construction team is supposed to have the skills to decide on sufficient rock support measures during construction. Whatever amount of support that is put in to ensure a safe working place, it would be the cheapest solution.<br>It is assumed that there is an established strategy for the principles to decide on the amount of support. | A conservative approach to rock support increase tunnel construction cost only marginal. |
| Geological characterization, installations, pilot hole drilling for deposition holes. | Work force in the tunnel is assumed to include staff with limited rock mechanics experience that has to move along the tunnel.<br>Unsupported sections require systematic inspection and scaling. Such activities can be carried out without disturbing the works. | There is a tentative risk for block fall. Risk is reduced with frequent scaling. |
| Drilling of deposition holes. | Work in the tunnel is more stationary. Drilling machine can have protective roof.<br>Some work force has to move along the tunnel.<br>Drilling generates heat, and consequently changes the boundary conditions (cf. Section 4.2). | Potential for increased risk for block fall due to thermal effect.<br>Risk is reduced with frequent scaling. |
| Characterization of deposition holes. | Work in the tunnel is stationary. Work in deposition holes can be protected by a roof. Some work force has to move along the tunnel. | Risk is reduced with frequent scaling. |
| Notch for the plug. | Work in the tunnel is more stationary and close to the tunnel collar. Machines generate some heat, might change boundary conditions. Machines can have protective roof. | Risk is reduced with local scaling. |
| Cleaning up, prepare for deposition. | Work is partly done by machines. Some work force has to move along the tunnel for removal of temporary infrastructure. | Risk is reduced with scaling. |
| Deposition – placing buffer and deposition of canister. | Placing buffer and deposition of canisters are done by remote control.<br>Some work force has to move along the tunnel. | Block fall would be an obstacle for deposition work. Risk for interruptions . |
| Backfiling (three shifts/day). | Current reference method for backfilling requires continuous work flow. Backfilling is highly automated, but require some work force to move along the tunnel. | Block fall would be an obstacle for backfilling work. Risk for interruptions. |
| Plugging of the backfilled tunnel. | Work in the tunnel is stationary and close to the tunnel collar. Machines and fresh concrete generates some heat, might change boundary conditions. Machines can have protective roof. | Risk is reduced with local scaling. |

Preventing fall of ground between spot bolts could be done by shotcrete or wire mesh. However, as stated earlier, the good rock conditions do not indicate the need for systematic support of all surfaces. It is likely that the rock surfaces can be subject for a number of inspections and maintenance scaling activities, because the rock construction works is estimated to need some 105 ± 10 weeks for a deposition tunnel. Nearby excavations might continue for example during deposition hole drilling and characterization activities. The lag time between different activities will also vary. This is the main reason for the operational life time to be up to ca 5 years.

The risk of taking wrong decision on support (too little support) has likely a larger consequence as the deposition and backfilling works comes closer. Any need for scaling for safety purposes during deposition and backfilling might have larger consequences than just the delay for scaling and cleaning up activities. Table 8-1 discuss and estimate the preliminary consequence and the consequence of taking too early or too late decision.

SKB need to develop a maintenance strategy. In the deposition area, the strategy needs to be adapted to logistics and deposition rate with preferred support installation before deposition.

Reporting and documentation of observed fall of ground should always be performed and the section and block size should be noted. It is therefore important that all personnel working underground are aware of this responsibility. Documentation of scaling activities must be carried out for each scaling occasion.

# 9 Recommendations

## 9.1 Support options in deposition tunnels

The work conducted this far suggests the following recommendations for the deposition tunnels:

- Based on experience from Äspö HRL it should be possible to reach the requirements stated by the Swedish Work Environment Authority with continuous maintenance scaling combined with selective rock support measures. This is also supported by the results of the numerical stress simulations. Due to the reference excavation method (drill and blast), the rock support will in most cases be installed in end of the blast rounds if this approach is applied.
- A toolbox of support solutions should to be established. The toolbox should contain maintenance scaling combined with support measures. The expected types of hazards are falls of small chips from stress related spalling or gravity driven blocks caused by natural or blast induced fractures. The proposed support types must be able to protect the personnel working in the deposition tunnels from both types of outbreaks, i.e. both spot and surface support measures needs to be taken. The toolbox should also contain support measures for unexpected rock conditions or fractured rock mass in deformation zones.
- Two types of surface support are recommended, wire mesh and shotcrete. Shotcrete is more efficient and easier to apply, however not recommended in larger volumes due to its ability to react chemically with the backfill material. If wire mesh is used there is a need for development and industrialization of the installation process.
- For support of loose blocks selective rock bolts are recommended together with mechanized scaling.
- SKB need to establish a policy for rock reinforcement and develop a maintenance strategy. In the deposition area, the strategy needs to be adapted to logistics and deposition rate with preferred support installation before deposition.

## 9.2 Need for further studies

Several issues need to be studied further before a toolbox of support solutions can be determined:

- The amount and types of acceptable rock support material that can be left in the deposition tunnels after closure should be determined.
- It needs to be determined to what extent low-pH shotcrete can be used in the deposition tunnels and in what locations, considering post closure safety.
- If wire mesh is to be applied in large scale in the deposition tunnels there will be a need for a further development of the production methods to install the mesh more cost effective.
- In order to better understand excavation damage the combined effect of dynamic loading from blasting and the induced stress field around the tunnel face should be studied for larger charge concentrations in the bottom charge.

# 10 References

SKB's (Svensk Kärnbränslehantering AB) publications can be found at www.skb.com/publications.


**Andersson C, Söderhäll J, 2001.** Rock mechanical conditions at the Äspö HRL. A study of the correlation between geology, tunnel maintenance and tunnel shape. SKB R-01-53, Svensk Kärnbränslehantering AB.

**Arbetsmiljöverket, 2010.** AFS 2010:1. Berg- och gruvarbete. Solna: Arbetsmiljöverket. (In Swedish.)

**Back P-E, Wrafter J, Sundberg J, Rosén L, 2007.** Thermal properties. Site descriptive modelling Forsmark – stage 2.2. SKB R-07-47, Svensk Kärnbränslehantering AB.

**Bodén A, Pettersson S, 2011.** Development of rock bolt grout and shotcrete for rock support and corrosion of steel in low-pH cementitous materials. SKB R-11-08, Svensk Kärnbränslehantering AB.

**Carlsson A, Christiansson R, 2007.** Construction experiences from underground works at Forsmark. Compilation report. SKB R-07-10, Svensk Kärnbränslehantering AB.

**Eriksson M, Petersson J, Danielsson P, Leander M, 2009.** Underground design Forsmark. Layout D2. Rock mechanics and rock support. SKB R-08-115, Svensk Kärnbränslehantering AB.

**Glamheden R, Fredriksson A, Röshoff K, Karlsson J, Hakami H, Christiansson R, 2007.** Rock mechanics Forsmark. Site descriptive modelling Forsmark stage 2.2. SKB R-07-31, Svensk Kärnbränslehantering AB.

**Goricki A, 2003.** Classification of rock mass behaviour based on hierarchical rock mass characterization for the design of underground structures. PhD thesis. Department of Civil Engineering, Graz University of Technology, Austria.

**Hardenby C, Sigurdsson O, 2010.** Äspö Hard Rock Laboratory. The TASS-tunnel. Geological mapping. SKB R-10-35, Svensk Kärnbränslehantering AB.

**Hoek E, Bawden W. F, Kaiser P K, 2000.** Support of underground excavations in hard rock. Rotterdam: Balkema.

**Holmgren J, 1979.** Punch-loaded shotcrete linings on hard rock. PhD thesis. Royal Institute of Technology, Stockholm, Sweden.

**Itasca, 2011.** FLAC – Fast lagrangian analysis of continua, user's guide. Minneapolis, MN: Itasca Consulting Group, Inc.

**Ittner H, 2009.** Äspö Hard Rock Laboratory. Evaluation of scaling records for TASA access tunnel. SKB IPR-10-01, Svensk Kärnbränslehantering AB.

**Ittner H, 2011.** Support design for deposition tunnels. Master thesis. Chalmers University of Technology, Gothenburg, Sweden.

**Karlzén R, Johansson E, 2010.** Slutrapport från drivningen av TASS-tunneln. SKB R-10-31, Svensk Kärnbränslehantering AB. (In Swedish.)

**Martin C D, 2007.** Quantifying in situ stress magnitudes and orientations for Forsmark. Forsmark stage 2.2. SKB R-07-26, Svensk Kärnbränslehantering AB.

**Nyberg U, Harefjord L, Bergman B, Christiansson R, 2008.** Äspö Hard Rock Laboratory. Monitoring of vibrations during blasting of the APSE tunnel. SKB R-05-27, Svensk Kärnbränslehantering AB.

**Olsson M, Markström I, Pettersson A, Sträng M, 2009.** Examination of the Excavation Damaged Zone in the TASS tunnel, Äspö HRL. SKB R-09-39, Svensk Kärnbränslehantering AB.

**SKB, 2007.** Final repository facility. Underground design premises/D2. SKB R-07-33, Svensk Kärnbränslehantering AB.

**SKB, 2009a.** Site engineering report Forsmark. Guidelines for Underground Design Step D2. SKB R-08-83, Svensk Kärnbränslehantering AB.

**SKB, 2009b.** Underground design Forsmark. Layout D2. SKB R-08-116, Svensk Kärnbränslehantering AB.

**Stephens M B, Fox A, La Pointe P, Simeonov A, Isaksson H, Hermanson J, Öhman J, 2007.** Geology Forsmark Site descriptive modelling Forsmark stage 2.2. SKB R-07-45, Svensk Kärnbränslehantering AB.

**Stigsson M, 2009.** Statistics of modelled conductive fractures based on Laxemar and Forsmark Site descriptive model data. SKB R-09-48, Svensk Kärnbränslehantering AB.

**Sundberg J, Back P-E, Bengtsson A, Ländell M, 2005.** Thermal modelling. Preliminary site description Forsmark area – version 1.2. SKB R-05-31, Svensk Kärnbränslehantering AB.

**Sundberg J, Wrafter J, Ländell M, Back P-E, Rosén L, 2008.** Thermal properties Forsmark. Modelling stage 2.3. Complementary analysis and verification of the thermal bedrock model, stage 2.2. SKB R-08-65, Svensk Kärnbränslehantering AB.

**Svensk byggtjänst, 1999.** Anläggnings AMA 98: allmän material- och arbetsbeskrivning för anläggningsarbeten. Stockholm: Svensk byggtjänst.

**Trafikverket, 2014.** Projektering av bergkonstruktioner. Report 2014:144, Swedish Transport Administration. (In Swedish.)

# Appendix 1

## A1.1 Results from numerical stress simulation in FLAC

**Table A1-1. The level of in plane induced stress for elements in unfavourably locations in the section 42 m. Likely level of in situ stress.**

| Model zone coordinates i,j | Model stage | Sigma 1 (max in xy plane) MPa | Sigma 2 (min in xy plane) MPa | Sigma zz (out-of-plane stress component) MPa |
|---|---|---|---|---|
| All | Initially (in situ stress conditions) | 23 | 13 | 41 |
| (269, 364) | After excavation | 148 | 20 | 71 |
| (269, 364) | After 6.3 days | 159 | 21 | 77 |
| (269, 365) | After excavation | 97 | 18 | 59 |
| (269, 365) | After 6.3 days | 104 | 19 | 64 |
| (270, 364) | After excavation | 116 | 10.5 | 62 |
| (270, 364) | After 6.3 days | 124 | 11.3 | 67 |
| (194, 362) | After excavation | 78 | 9.5 | 53 |
| (194, 362) | After 6.3 days | 84 | 10 | 87 |
| (195, 361) | After excavation | 110 | 2.1 | 59 |
| (195, 361) | After 6.3 days | 118 | 2 | 63 |
| (260, 363) | After excavation | 19 | 1.3 | 37 |
| (260, 363) | After 6.3 days | 21 | 0.1 | 40 |

**Table A1-2. The level of in plane induced stress for elements in unfavourably locations in the section 77 m. Likely level of in situ stress.**

| Model zone coordinates i,j | Model stage | Sigma 1 (max in xy plane) MPa | Sigma 2 (min in xy plane) MPa | Sigma zz (out-of-plane stress component) MPa | Differenc between Sigma 1 and Sigma 2 (in the plane) MPa |
|---|---|---|---|---|---|
| **Concave geometry elements** | | | | | |
| (326, 345) | After excavation | 88 | 10 | 55 | 78 |
| (326, 345) | After 5.6 days | 98 | 11 | 61 | 87 |
| (326, 346) | After excavation | 63 | 10 | 45 | 53 |
| (326, 346) | After 5.6 days | 71 | 11 | 54 | 59.4 |
| (350, 319) | After excavation | 45 | 17 | 47 | 28 |
| (350, 319) | After 5.6 days | 52 | 20 | 52 | 33 |
| (312, 12) | After excavation | 105 | 11 | 60 | 94 |
| (312, 12) | After 5.6 days | 116 | 12.5 | 65 | 103 |
| **Convex geometry elements** | | | | | |
| (347, 39) | After excavation | 1.8 | 0.5 | 33 | 1.3 |
| (347, 39) | After 5.6 days | 2.1 | 0.6 | 36 | 1.5 |
| (106, 168) | After excavation | 0.81 | 0.015 | 32.9 | 0.8 |
| (106, 168) | After 5.6 days | 2.01 | 0.06 | 36.1 | 2.0 |
| (105, 168) | After excavation | 1.05 | 0.005 | 33.0 | 1.0 |
| (105, 168) | After 5.6 days | 2.2 | 0.05 | 36.1 | 2.1 |
| (104, 168) | After excavation | 1.4 | 0.023 | 33.0 | 1.4 |
| (104, 168) | After 5.6 days | 2.5 | 0.017 | 36.2 | 2.5 |
| (97, 151) | After excavation | 10.9 | 1.0 | 35.5 | 9.8 |
| (97, 151) | After 5.6 days | 17.4 | 1.8 | 40.1 | 15.6 |

**Table A1-3. The level of in plane induced stress for elements in unfavourably locations in the section 77 m. Situation with maximum in situ stress.**

| Model zone coordinates i,j | Model stage | Sigma 1 (max in xy plane) MPa | Sigma 2 (min in xy plane) MPa | Sigma zz (out-of-plane stress component) MPa | Differenc between Sigma 1 and Sigma 2 (in the plane) MPa |
|---|---|---|---|---|---|
| **Concave geometry elements** | | | | | |
| (326, 345) | After excavation | 157.5 | 18 | 89.5 | 140 |
| (326, 345) | After 5.6 days | 168 | 19 | 95 | 149 |
| (326, 346) | After excavation | 113 | 18 | 79 | 95 |
| (326, 346) | After 5.6 days | 120 | 19 | 84 | 101 |
| (350, 319) | After excavation | 64 | 24 | 69 | 40 |
| (350, 319) | After 5.6 days | 71 | 26 | 74 | 45 |
| (312, 12) | After excavation | 207 | 22 | 102 | 184 |
| (312, 12) | After 5.6 days | 217 | 23 | 107 | 194 |
| **Convex geometry elements** | | | | | |
| (347, 39) | After excavation | 3.0 | 0.8 | 50 | 2.1 |
| (347, 39) | After 5.6 days | 3.2 | 0.9 | 53 | 2.3 |
| (106, 168) | After excavation | −0.16 | −4.1 | 48 | 3.9 |
| (106, 168) | After 5.6 days | −0.11 | −2.9 | 51 | 2.8 |
| (105, 168) | After excavation | −0.17 | −3.2 | 48.3 | 3.1 |
| (105, 168) | After 5.6 days | −0.13 | −2.1 | 51.5 | 2.0 |
| (104, 168) | After excavation | −0.06 | −3.0 | 48.4 | 2.9 |
| (104, 168) | After 5.6 days | −0.05 | −1.8 | 51.6 | 1.8 |
| (97, 151) | After excavation | −1.6 | −12.8 | 45.8 | 11.2 |
| (97, 151) | After 5.6 days | −0.81 | −6.4 | 50.4 | 5.6 |

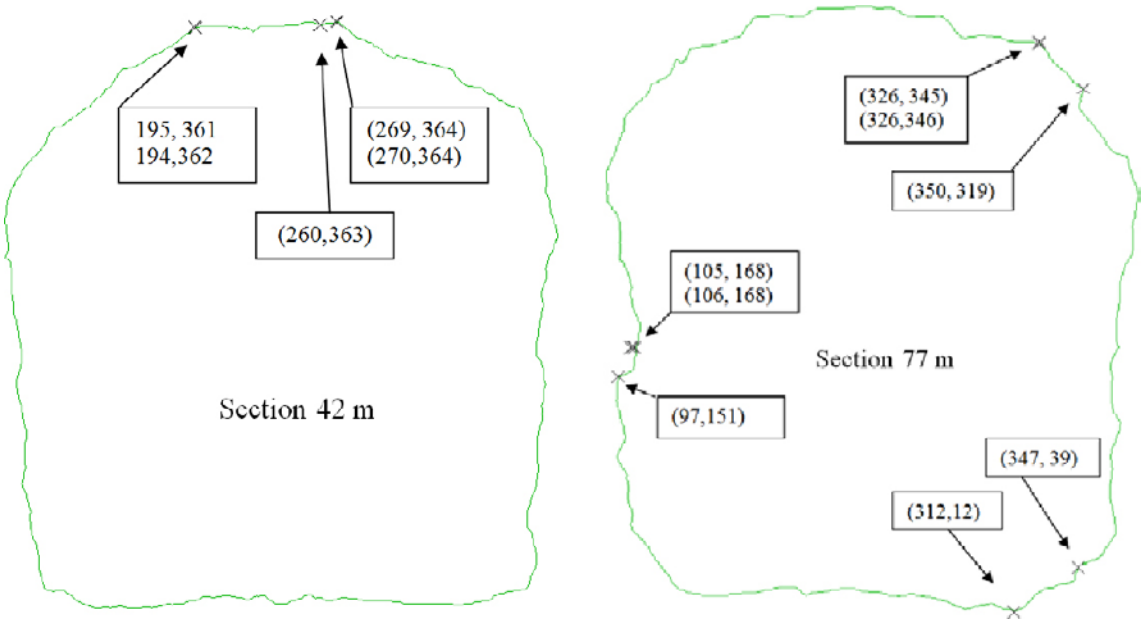


***Figure A1-1.*** *Location of studied elements in the sections 42 m and 77 m.*

## A1.2 Mesh set up for simulation of induced stress from thermal loads

The Figure A1-2 shows the mesh in section 42 m. Boundary condition was set to no displacements on boundary. Figure A1-3 shows the mesh for the section 77 m.

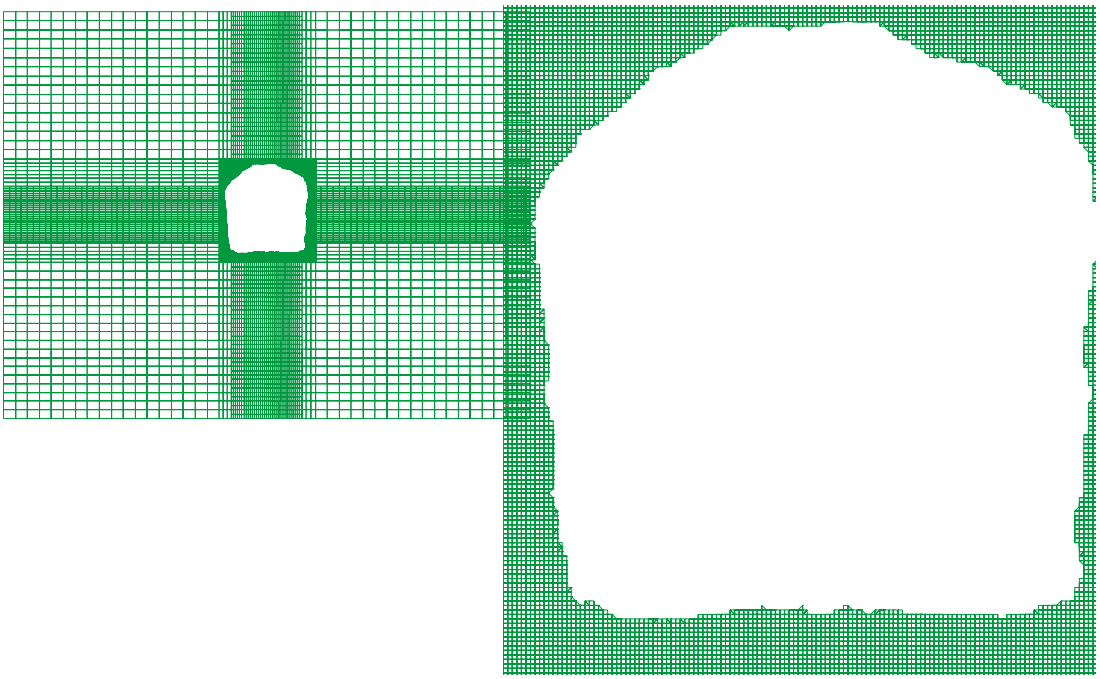

***Figure A1-2.*** *Left: the mesh for the section 42 m. Right: detail of the mesh close to the contour.*

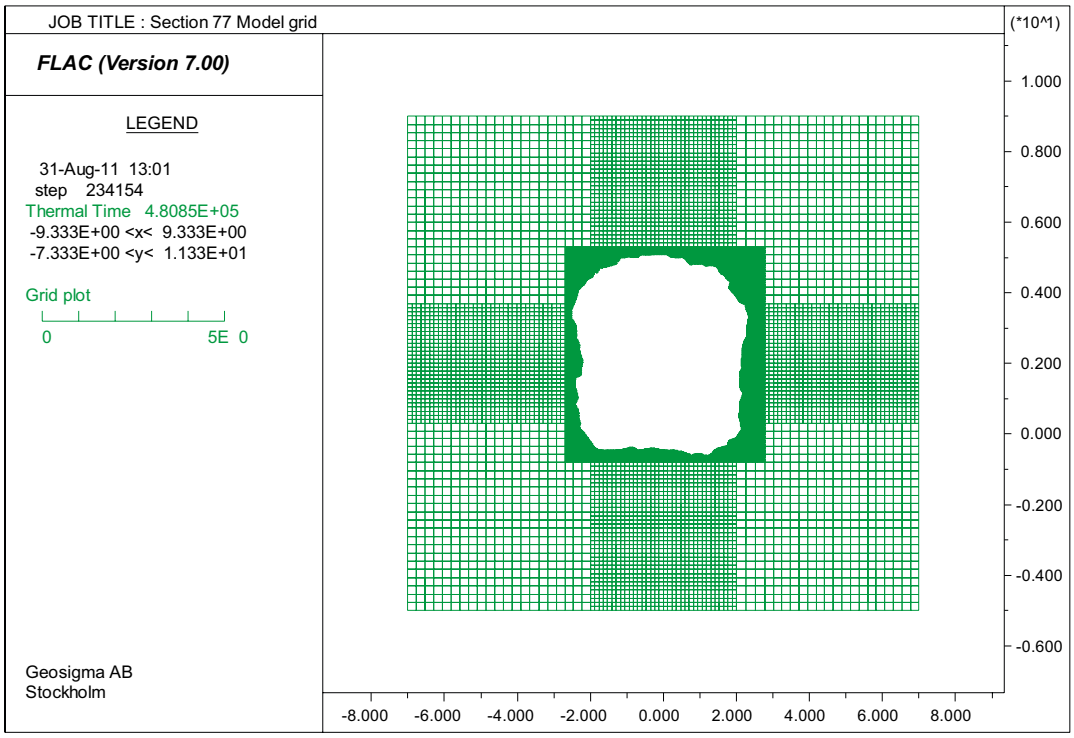


***Figure A1-3.*** *The mesh for the section 77 m.*

## A1.3 Stress plots of induced stress from thermal loads

The Figures A1-4 to A1-7 depicts the results of 6.3 days of heating. Close to the boundary most of the stress increase is obtained early in the warming period.

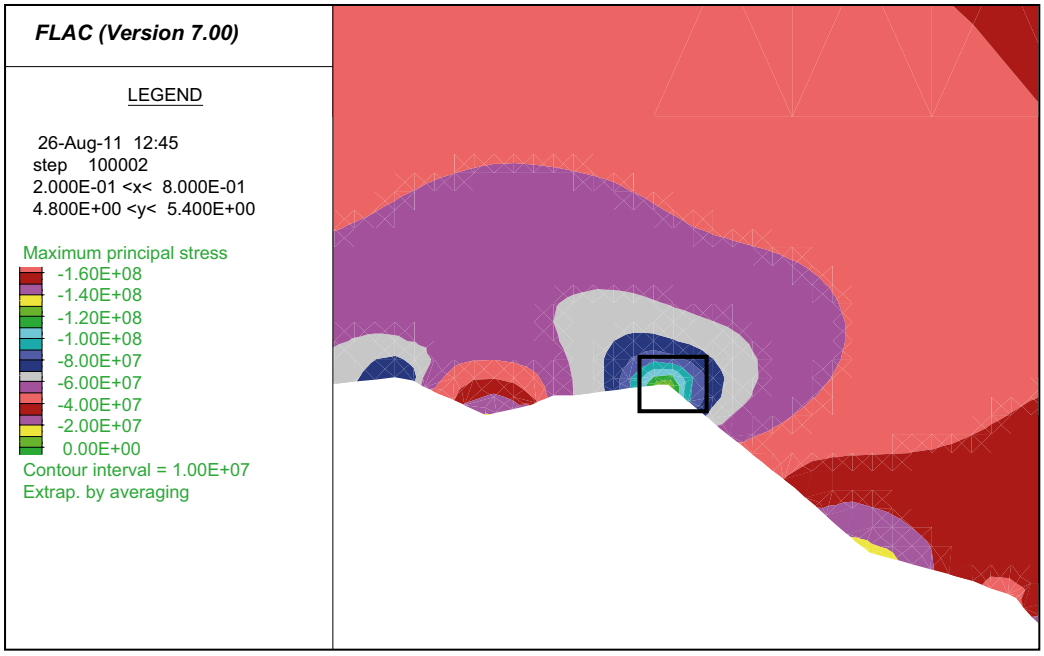


***Figure A1-4.*** *Induced stress in the x-y plane in a roof detail of section 42 m after excavation. Most likely level of in situ stress.*

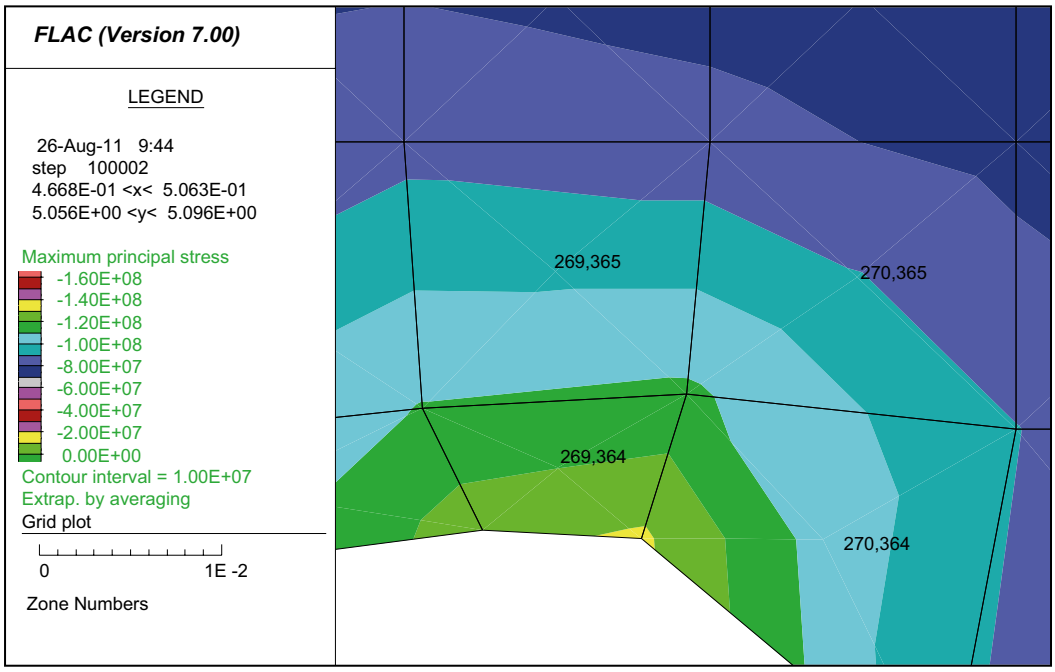


***Figure A1-5.*** *Induced stress in the x-y plane in a roof detail of section 42 m after excavation. Most likely level of in situ stress.*

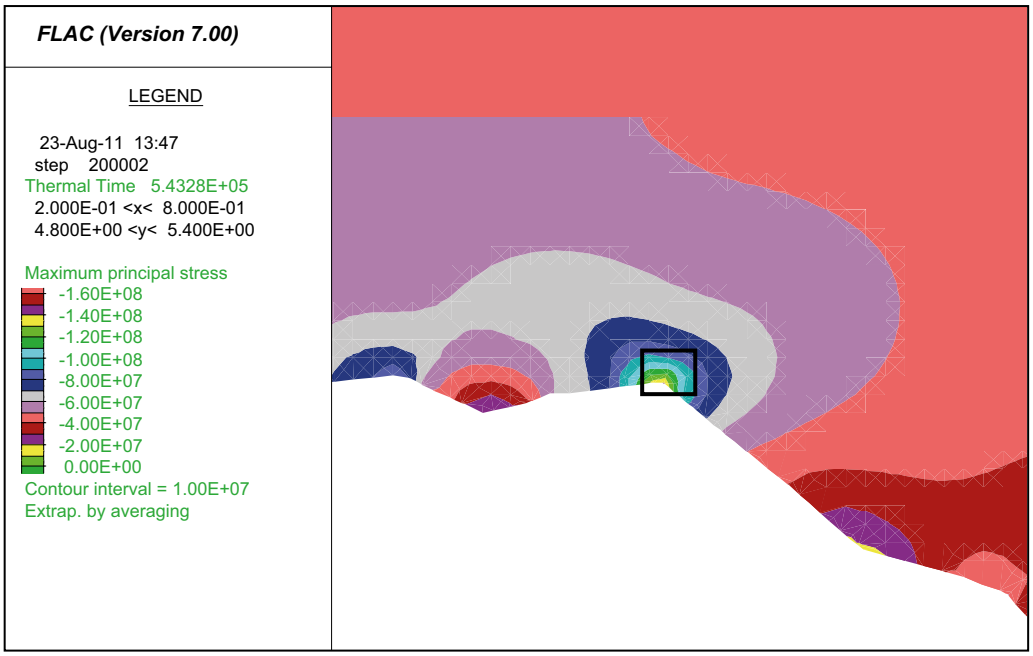


***Figure A1-6.*** *Induced stress in the x-y plane in a roof detail of section 42 m after heating. Situation with maximum in situ stress.*

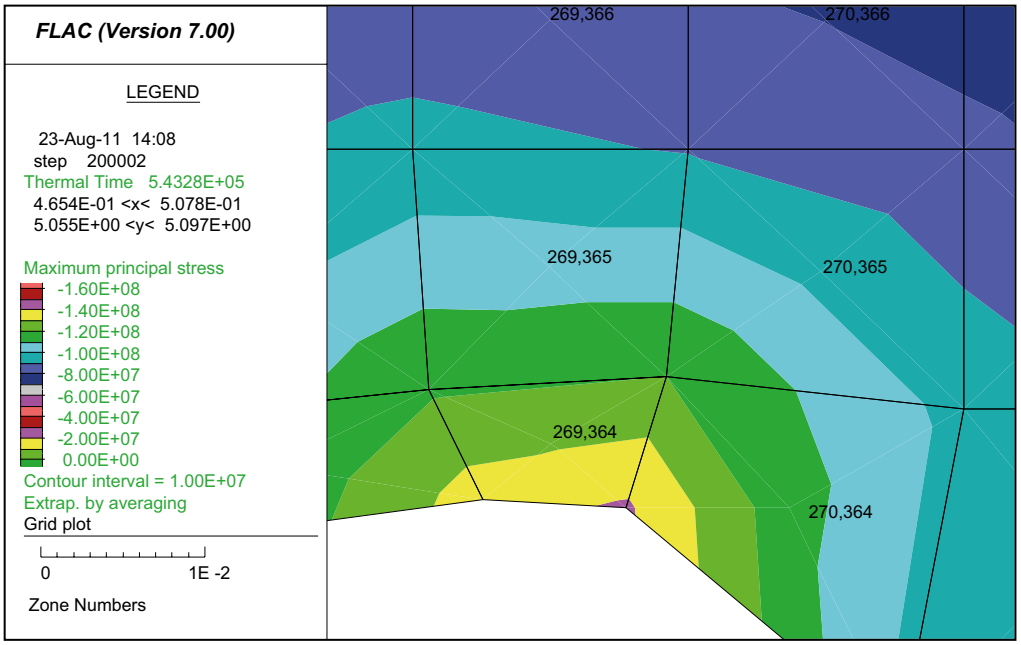


***Figure A1-7.*** *Induced stress in the x-y plane in a roof detail of section 42 m after heating. Situation with maximum in situ stress.*

### A1.3.1 Plots of elastic dicplacements from thermal loads

Elastic dicplacements due to 6 days of warming with 17 °C on the excavation boundary are of small magnitudes up to 0.03 mm. The Figures 8 and 9 presents dicplacement magnitudes separated in x and y directions of the x-y plane.

Figure A1-10 shows accumulated displacement from excavation and heating in a roof element of section 42 m.

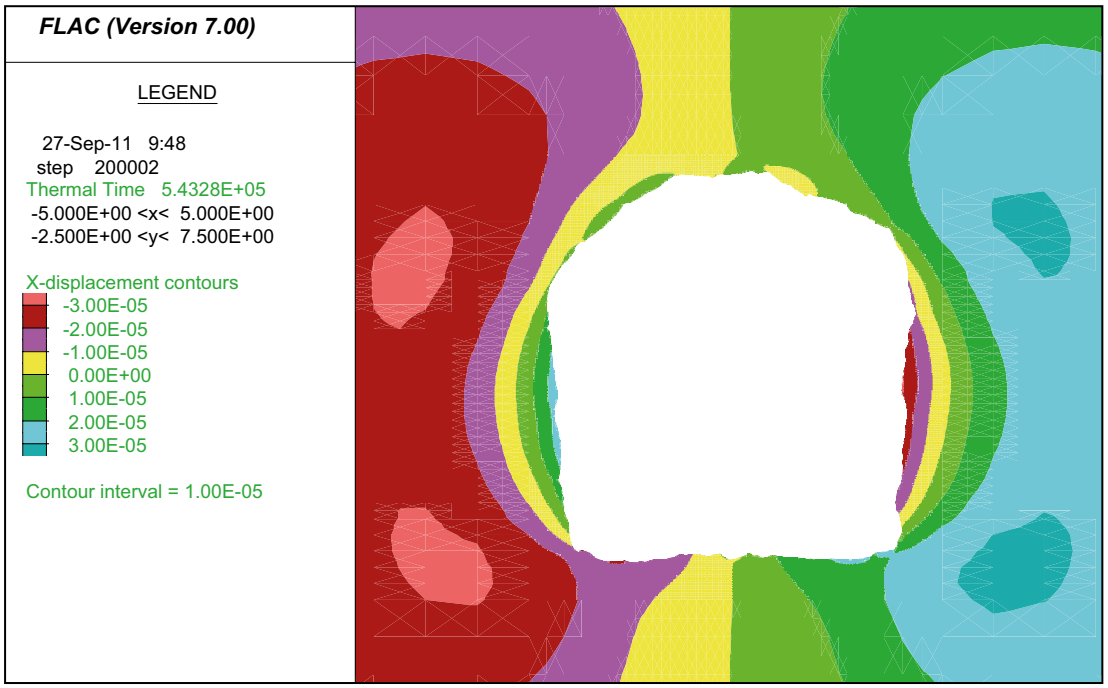


***Figure A1-8.*** *Magnitudes of elastic displacements in the x-direction due to 6 days of heating for the section 42 m.*

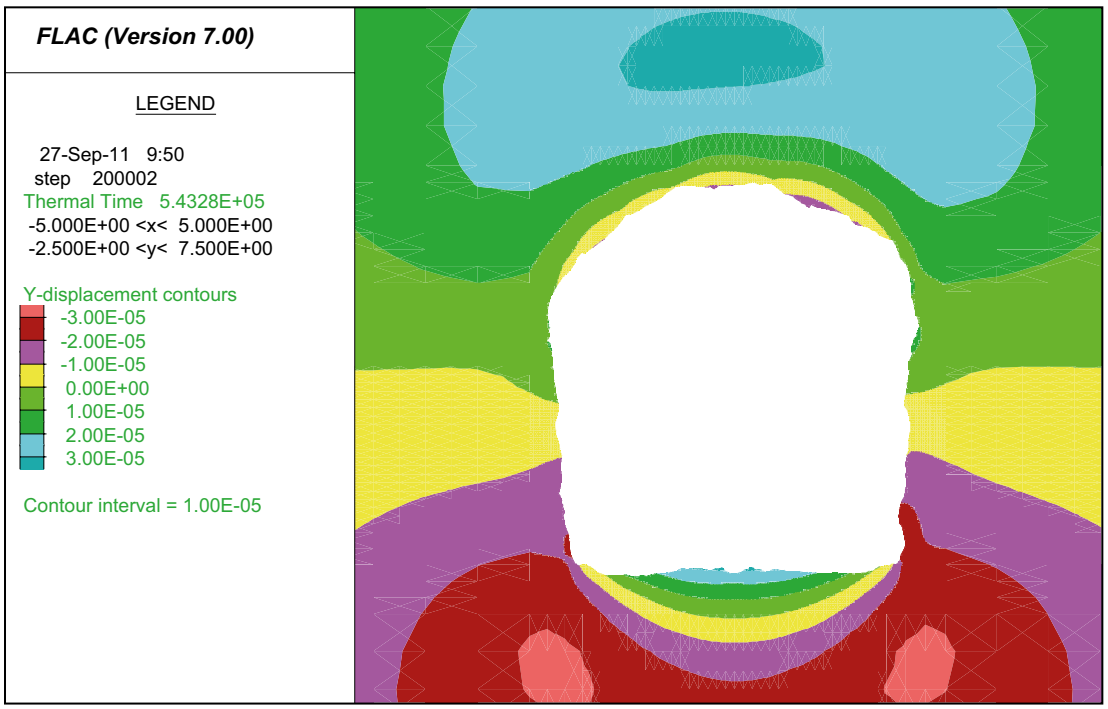


***Figure A1-9.*** *Magnitudes of elastic displacements in the y-direction due to 6 days of heating for the section 42 m.*

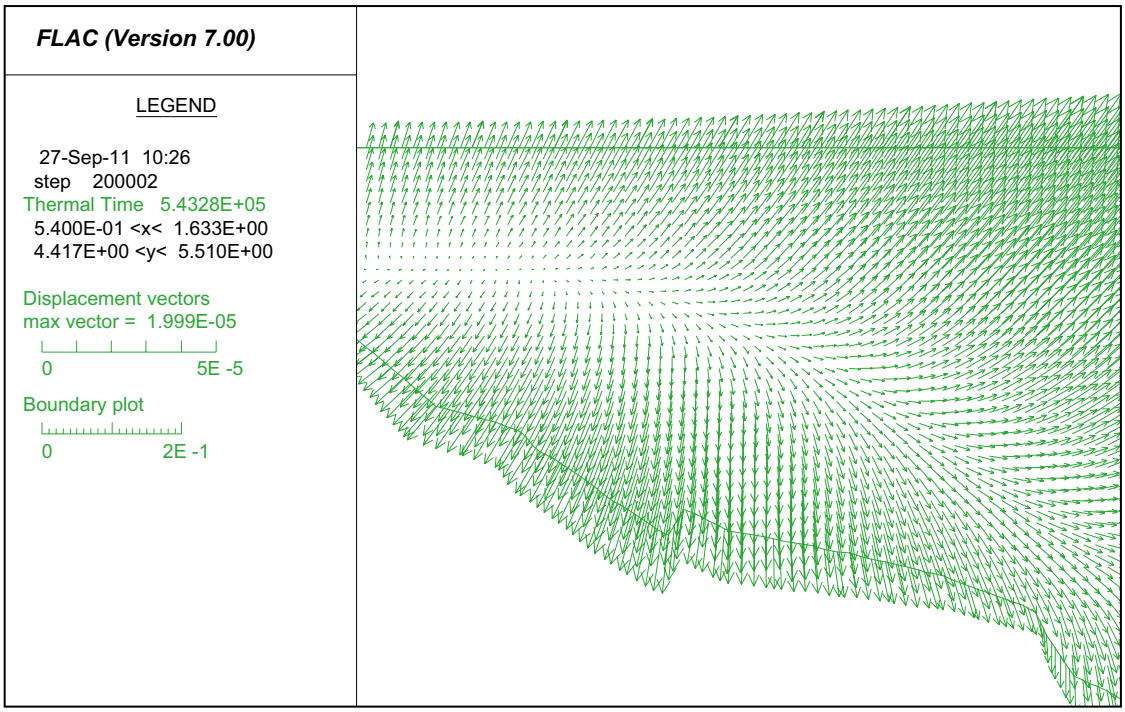


***Figure A1-10.*** *Elastic displacement vectors in a roof element of section 42 m.*